2

Braids, Knots, and Links

In this chapter we study the relationship between braids, knots, and links. Throughout the chapter, we denote by I the closed interval $[0,1]$ in $\mathbf{R}$.

2.1 Knots and links in three-dimensional manifolds

We briefly discuss the notions from knot theory needed for the sequel. For detailed expositions of knot theory, the reader is referred to the monographs [BZ85], [Kaw96], [Mur96], [Rol76].

2.1.1 Basic definitions

Let M be a 3-dimensional topological manifold, possibly with boundary ∂M. A *geometric link* in M is a locally flat closed 1-dimensional submanifold of M. Recall that a manifold is *closed* if it is compact and has an empty boundary. A closed 1-dimensional submanifold $L \subset M$ is *locally flat* if every point of L has a neighborhood $U \subset M$ such that the pair $(U, U \cap L)$ is homeomorphic to the pair $(\mathbf{R}^3, \mathbf{R} \times \{0\} \times \{0\})$. This condition implies that $L \subset M^\circ = M - \partial M$ and excludes all kinds of locally wild behavior of L inside M°.

Being a closed 1-dimensional manifold, a geometric link in M must consist of a finite number of components homeomorphic to the standard unit circle

$$S^1 = \{z \in \mathbf{C} \,|\, |z| = 1\}\,.$$

A space homeomorphic to S^1 is called a (topological) circle. A geometric link consisting of $n \geq 1$ circles is called an *n-component link*. For example, the boundary of n disjoint embedded 2-disks in M° is a *trivial n-component link* in M.

One-component geometric links are called *geometric knots*. Examples of nontrivial knots and links in $\mathbf{R}^3$ are shown in Figure 2.1, which presents the trefoil knot, the figure-eight knot, and the Hopf link.

C. Kassel, V. Turaev, *Braid Groups*, DOI: 10.1007/978-0-387-68548-9_2,

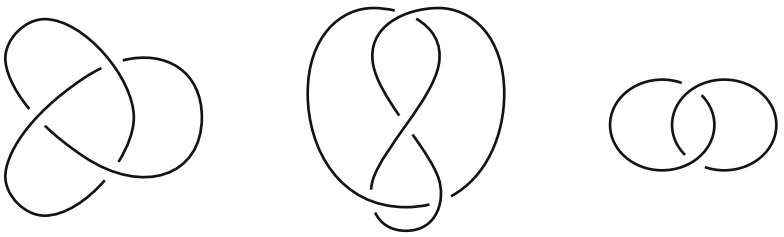

Fig. 2.1. Knots and links in $\mathbf{R}^3$

Two geometric links L and L' in M are *isotopic* if L can be deformed into L' by an isotopy of M into itself. Here by an *isotopy* of M (into itself), we mean a continuous family of homeomorphisms $\{F_s : M \to M\}_{s\in I}$ such that $F_0 = \mathrm{id}_M : M \to M$. The continuity of this family means that the mapping $I \to \mathrm{Top}(M)$, $s \mapsto F_s$ is continuous or, equivalently, the mapping

$$M \times I \to M\,, \quad (x, s) \mapsto F_s(x)\,,$$

where $x \in M, s \in I$, is continuous; see Section 1.7.1. An isotopy $\{F_s\}_{s\in I}$ of M is said to be an *isotopy of L into L'* if $F_1(L) = L'$. The links L and L' are isotopic if there is an isotopy of L into L'. Isotopic geometric links have the same number of components. In other words, the number of components is an isotopy invariant of geometric links.

The relation of isotopy is obviously an equivalence relation in the class of geometric links in M. The corresponding equivalence classes are called *links* in M. The links having only one component are called *knots*. The ultimate goal of knot theory is a classification of knots and links.

If M has a smooth structure, then any geometric link in M is isotopic to a geometric link whose underlying 1-dimensional manifold is a smooth submanifold of M. Therefore working with links in smooth 3-dimensional manifolds, we can always restrict ourselves to smooth representatives.

2.1.2 Link diagrams

The technique of braid diagrams discussed in Chapter 1 can be extended to links. We shall restrict ourselves to the case in which the ambient 3-manifold is the product of a surface Σ (possibly with boundary $\partial\Sigma$) with I. For $n \geq 1$, a *link diagram* on Σ with n components is a set $\mathcal{D} \subset \Sigma - \partial\Sigma$ obtained as a union of n circles with a finite number of intersections and self-intersections such that each (self-)intersection is a meeting point of exactly two branches of $\mathcal{D}$, one of these branches being distinguished and called *undergoing*, the other one being *overgoing*. In a neighborhood of a point, $\mathcal{D}$ looks like a straight line in $\mathbf{R}^2$ or like the set $\{(x, y) \,|\, xy = 0\} \subset \mathbf{R}^2$, where one of the branches $x = 0, y = 0$ is distinguished. The circles forming $\mathcal{D}$ are called the *components* of $\mathcal{D}$. The (self-)intersections of these circles are called *crossings* or *double points* of $\mathcal{D}$. Note that three components of $\mathcal{D}$ never meet in a point.

The branch of a link diagram going under a crossing is graphically represented by a broken line. The pictures in Figure 2.1 can be considered as link diagrams in the plane.

Each link diagram $\mathcal{D}$ on a surface Σ presents a link

$$L(\mathcal{D}) \subset \Sigma \times I.$$

It is obtained from $\mathcal{D} \subset \Sigma = \Sigma \times \{1/2\}$ by pushing the undergoing branches into $\Sigma \times [1/2, 1)$. The link $L(\mathcal{D})$ is well defined up to isotopy.

Observe that any link in $\Sigma \times I$ can be presented by a link diagram on Σ. To see this, represent the given link by a geometric link $L \subset \Sigma \times I$ whose projection to Σ has only double transversal crossings. At each of the crossings choose the undergoing branch to be the one that comes from the subarc of L with bigger I-coordinate. This gives a link diagram on Σ representing the isotopy class of L.

Two link diagrams $\mathcal{D}$ and $\mathcal{D}'$ on Σ are *isotopic* if there is an isotopy of Σ into itself transforming $\mathcal{D}$ into $\mathcal{D}'$. More precisely, $\mathcal{D}$ and $\mathcal{D}'$ are *isotopic* if there is a continuous family of homeomorphisms $\{F_s : \Sigma \to \Sigma\}_{s \in I}$ such that $F_0 = \mathrm{id}_\Sigma$ and $F_1(\mathcal{D}) = \mathcal{D}'$. It is understood that F_1 maps the crossings of $\mathcal{D}$ to the crossings of $\mathcal{D}'$, preserving the under/overgoing data. Clearly, if $\mathcal{D}$ and $\mathcal{D}'$ are isotopic, then $L(\mathcal{D})$ and $L(\mathcal{D}')$ are isotopic in $\Sigma \times I$.

The transformations of link diagrams $\Omega_1, \Omega_2, \Omega_3$ shown in Figures 1.5a, 1.5b, and 2.2 below (as well as the inverse transformations) are called *Reidemeister moves*. These moves affect only a part of the diagram lying in a disk in Σ and preserve the rest of the diagram. Note that to apply these moves, we identify the disk in Σ with a disk in the plane of the pictures. If Σ is oriented, then we use only identifications transforming the orientation of Σ into the counterclockwise orientation in the plane of the pictures. For nonoriented Σ, we use arbitrary identifications.

In comparison to the theory of braid diagrams, we need here two additional moves Ω_1 shown in Figure 2.2. These moves add a "curl" or "kink" to the diagram. The inverse moves Ω_1^{-1} remove such kinks from link diagrams. On the other hand, in the setting of link diagrams, one Ω_2-move is sufficient: the two Ω_2-moves in Figure 1.5a can be obtained from each other by an isotopy in Σ rotating a small 2-disk in Σ affected by the move to an angle of 180°.

The classical Reidemeister theorem for link diagrams on $\mathbf{R}^2$ generalizes to diagrams on Σ: two link diagrams on Σ represent isotopic links in $\Sigma \times I$ if and only if these diagrams are related by a finite sequence of isotopies and Reidemeister moves $\Omega_1^{\pm 1}, \Omega_2^{\pm 1}, \Omega_3^{\pm 1}$. Indeed, any isotopy of a geometric link in $\Sigma \times I$ may be split as a composition of a finite number of "local" isotopies changing the link only inside a cylinder of type $U \times I$, where U is a small open disk in Σ. Since the pair $(U \times I,\, U \times \{1/2\})$ is homeomorphic to the pair $(\mathbf{R}^2 \times I,\, \mathbf{R}^2 \times \{1/2\})$, we can apply the standard Reidemeister theory to the part of the link diagram lying in U. This implies that under such a local isotopy the diagram is changed via a sequence of moves $\Omega_1^{\pm 1}, \Omega_2^{\pm 1}, \Omega_3^{\pm 1}$.

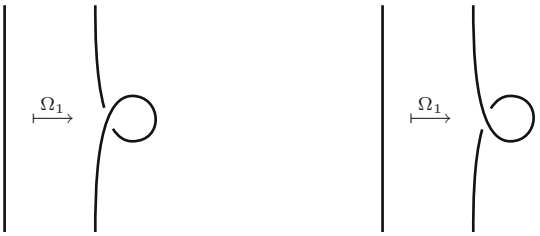

Fig. 2.2. The moves Ω_1

2.1.3 Ordered and oriented links

Links admit a number of natural additional structures. Here we describe two such structures: order and orientation. An n-component geometric link is *ordered* if its components are numbered by $1, 2, \ldots, n$. By *isotopies* of ordered links, we mean order-preserving isotopies. The order is easily exhibited on link diagrams: it suffices to attach the numbers $1, 2, \ldots, n$ to the components of the diagram and to keep these numbers unchanged under isotopy.

An *orientation* of a geometric link L in a 3-dimensional manifold M is an orientation of the underlying 1-dimensional manifold L. In the figures, the orientation is indicated by arrows on the link components. By *isotopies* of oriented links, one means orientation-preserving isotopies. Each oriented link $L \subset M$ is a 1-cycle and represents a homology class

$$[L] \in H_1(M) = H_1(M; \mathbf{Z}) .$$

This class is an isotopy invariant of L. Indeed, the components of two isotopic oriented links are pairwise homotopic and consequently pairwise homologous.

To exhibit the orientation of the link presented by a link diagram on a surface it suffices to orient all components of the diagram. Each Reidemeister move gives rise to several *oriented Reidemeister moves* on oriented link diagrams keeping the orientations of the strands. Specifically, orienting all the strands in Figure 2.2 in the same direction (up or down), we obtain four oriented Ω_1-moves. Similarly, the two moves Ω_2 in Figure 1.5a give rise to eight oriented Ω_2-moves. In two of them, both strands are directed down (before and after the move). These two oriented Ω_2-moves are said to be *braidlike* and are denoted by Ω_2^{br}. The two oriented Ω_2-moves in which the strands are directed up can be expressed as compositions of Ω_2^{br} and isotopies rotating a 2-disk by the angle 180°. The remaining oriented Ω_2-moves, in which the strands are directed in opposite directions, are said to be *nonbraidlike*. In a similar way, the move Ω_3 in Figure 1.5b gives rise to eight oriented Ω_3-moves. Any seven of them can be expressed as compositions of the eighth move and oriented Ω_2-moves (see [Tur88] or [Tra98]). Therefore it is enough to consider only the oriented Ω_3-move in which all three strands are directed down. This move is said to be *braidlike* and is denoted by Ω_3^{br}.

The Reidemeister theorem mentioned at the end of Section 2.1.2 implies that two oriented link diagrams on a surface Σ present isotopic oriented links in $\Sigma \times I$ if and only if these diagrams are related by a finite sequence of orientation-preserving isotopies and oriented Reidemeister moves.

2.1.4 The linking number

As an application of link diagrams, we define the integral linking number of knots in $\Sigma \times I$, where Σ is an arbitrary oriented surface (for nonoriented Σ, the linking number is defined only mod 2). Let L_1, L_2 be disjoint oriented knots in $\Sigma \times I$. Let us present the ordered oriented 2-component link $L_1 \cup L_2$ by a diagram on Σ. Let l^+ (resp. l^-) be the number of crossings of this diagram where a strand representing L_1 goes over a strand representing L_2 from left to right (resp. from right to left). Here the left and right sides of an oriented strand s are defined by the condition that the pair (a positively oriented vector tangent to s, a vector directed from the right of s to the left of s) determines the orientation of Σ. It is straightforward to check that the *linking number*

$$\mathrm{lk}(L_1, L_2) = l^+ - l^- \in \mathbf{Z}$$

is invariant under isotopies and oriented Reidemeister moves in the diagram. Hence $\mathrm{lk}(L_1, L_2)$ is a well-defined isotopy invariant of the link $L_1 \cup L_2$.

Exercise 2.1.1. Prove that an arbitrary geometric knot L in an orientable 3-dimensional manifold has an open neighborhood $U \supset L$ such that the pair (U, L) is homeomorphic to $(\mathbf{R}^2 \times S^1, \{x\} \times S^1)$, where $x \in \mathbf{R}^2$.

Exercise 2.1.2. Prove that two oriented link diagrams on $\mathbf{R}^2$ isotopic in the 2-sphere $S^2 = \mathbf{R}^2 \cup \{\infty\}$ represent isotopic oriented links in $\mathbf{R}^3$. (Hint: It suffices to verify this for an isotopy pushing a branch of the diagram across the point $\infty \in S^2$.)

Exercise 2.1.3. For any oriented surface Σ and any two disjoint oriented knots $L_1, L_2 \subset \Sigma \times I$,

$$\mathrm{lk}(L_1, L_2) - \mathrm{lk}(L_2, L_1) = [L_1] \cdot [L_2]\,,$$

where $[L_1] \cdot [L_2] \in \mathbf{Z}$ is the intersection number of $[L_1], [L_2] \in H_1(\Sigma)$. (Hint: This equality is obvious if

$$L_1 \subset \Sigma \times [0, 1/2]\,, \quad L_2 \subset \Sigma \times [1/2, 1]$$

and is preserved when a branch of L_1 is pushed across a branch of L_2.) Deduce that if Σ embeds in S^2, then $\mathrm{lk}(L_1, L_2) = \mathrm{lk}(L_2, L_1)$.

2.2 Closed braids in the solid torus

We introduce certain links in the solid torus, called closed braids, and classify them in terms of braids.

2.2.1 Solid tori

By a *solid torus*, we mean the product $V = D \times S^1$, where D is a closed 2-disk and $S^1 = \{z \in \mathbf{C} \,|\, |z| = 1\}$. The solid torus V is a compact connected orientable 3-dimensional manifold with boundary

$$\partial V = \partial D \times S^1 \approx S^1 \times S^1 \,.$$

Clearly,

$$V^\circ = V - \partial V = D^\circ \times S^1 \,,$$

where $D^\circ = D - \partial D$. The solid torus naturally arises in knot theory as a closed regular neighborhood of any knot in an orientable 3-dimensional manifold. Using a homeomorphism $D \approx I \times I$, we obtain

$$V \approx I \times I \times S^1 \approx S^1 \times I \times I \,.$$

The technique of link diagrams of Section 2.1 allows us to present links in V by diagrams on the annulus $S^1 \times I$.

2.2.2 Closed braids

A geometric link L in the solid torus $V = D \times S^1$ is called a *closed n-braid* with $n \geq 1$ if L meets each 2-disk $D \times \{z\}$ with $z \in S^1$ transversely in n points. It is clear that the projection on the second factor $V \to S^1$ restricted to L yields an (unramified) n-fold covering $L \to S^1$. We shall always provide L with the *canonical orientation* obtained as the lift of the counterclockwise orientation on S^1. Thus, a point moving along a component of L in the positive direction projects to a point moving along S^1 counterclockwise without ever stopping or going backward. The homology class $[L] \in H_1(V) = \mathbf{Z}$ of the oriented link $L \subset V$ is computed by $[L] = n\,[\{x\} \times S^1]$ for any $x \in D$.

For example, if Q is a finite subset of D°, then the link $Q \times S^1 \subset V$ is a closed n-braid, where $n = \mathrm{card}(Q)$. A closed 3-braid is drawn in Figure 2.3. Our interest in closed braids is due to their connection with braids. This connection will be discussed in the next subsections.

Two closed braids in V are *isotopic* if they are isotopic as oriented links. Note that the intermediate links appearing during an isotopy are not required to be closed braids. By abuse of language, isotopy classes of closed braids in V will be also called closed braids in V.

In general, a link in V is not isotopic to a closed braid in V. For instance, a link lying inside a small 3-ball in V is never isotopic to a closed braid. More generally, an oriented link in V homological to $m\,[\{x\} \times S^1]$ with $m \leq 0$, $x \in D$ is not isotopic to a closed braid in V. Another obstruction will be discussed in Exercise 2.2.4.

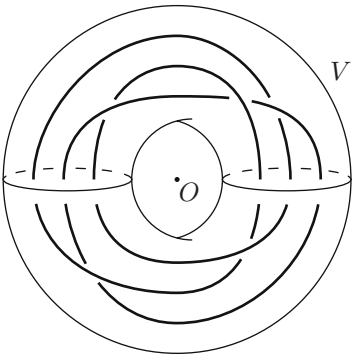

Fig. 2.3. A closed 3-braid in V

2.2.3 Closure of braids

Every braid β on n strings gives rise to a closed n-braid in the solid torus as follows. Fix a closed Euclidean disk $D \subset \mathbf{R}^2$ containing the set $Q = \{(1,0),(2,0),\dots,(n,0)\}$ in its interior. Observe that the solid torus $V = D \times S^1$ can be obtained from the cylinder $D \times I$ by the identification $(x,0) = (x,1)$ for all $x \in D$. (Here we identify $I/\partial I$ with S^1 via the standard homeomorphism $t \mapsto \exp(2\pi i t) : I/\partial I \to S^1$.) Pick a geometric braid $b \subset D^\circ \times I$ representing β (for the existence of such b, see Exercise 1.2.4). Let $\widehat{b} \subset V$ be the image of b under the projection $D \times I \to V$. It is obvious that $\widehat{b}$ is a closed n-braid in V. The canonical orientation of $\widehat{b}$ is determined by the direction on b leading from $Q \times \{0\}$ to $Q \times \{1\}$. If $b' \subset D \times I$ is another geometric braid representing β, then b is isotopic to b' in $D \times I$ (cf. Exercise 1.2.5). By (the proof of) Theorem 1.40, there is an isotopy of $D \times I$ constant on the boundary and transforming b into b'. This isotopy induces an isotopy between $\widehat{b}$ and $\widehat{b'}$ in V. Therefore the isotopy class of $\widehat{b}$ depends only on β. This class is called the *closure* of β and denoted by $\widehat{\beta}$.

Note that any closed n-braid $L \subset V$ is isotopic to $\widehat{\beta}$ for a certain $\beta \in B_n$. Indeed, we can deform L in the class of closed braids so that

$$L \cap (D \times \{1\}) = Q \times \{1\}\,.$$

Cutting V open along $D \times \{1\}$, we obtain a braid in $D \times I$ with closure L.

The description of $\widehat{\beta}$ given above is somewhat awkward from the point of view of drawing pictures. The following equivalent description is often more convenient. Observe that gluing two copies of $D \times I$ along $D \times \partial I = D \times \{0,1\}$, we again obtain V. Gluing a geometric braid representing β in the first $D \times I$ with the trivial braid $Q \times I$ in the second $D \times I$, we obtain $\widehat{\beta}$; see Figure 2.4. A link diagram in $S^1 \times I$ presenting $\widehat{\beta}$ is obtained by closing a diagram of β as in Figure 2.5.

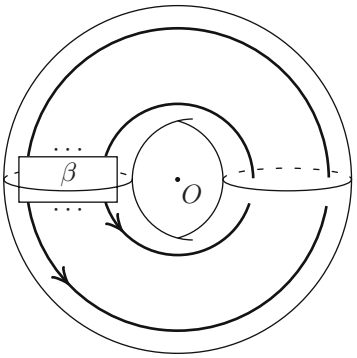

Fig. 2.4. Closing a braid β

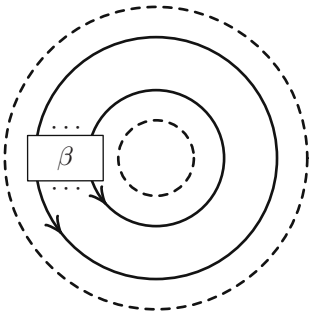

Fig. 2.5. A diagram of $\widehat{\beta}$

Theorem 2.1. *For any $n \geq 1$ and any β, $\beta' \in B_n$, the closed braids $\widehat{\beta}$, $\widehat{\beta'}$ are isotopic in the solid torus if and only if β and β' are conjugate in B_n.*

Theorem 2.1 gives an isotopy classification of closed n-braids in the solid torus: the isotopy classes of closed n-braids correspond bijectively to the conjugacy classes in B_n. In particular, any conjugacy invariant of elements of B_n determines an isotopy invariant of closed n-braids. For instance, the characteristic polynomial of a finite-dimensional linear representation of B_n yields an invariant of closed n-braids. Theorem 2.1 raises the problem of finding an algorithm to decide whether two given elements of B_n are conjugate. We shall address this problem in Chapter 6.

2.2.4 Proof of Theorem 2.1

Observe first that conjugate elements of B_n give rise to isotopic closed braids. In other words, $\widehat{\alpha\beta\alpha^{-1}} = \widehat{\beta}$ for any $\alpha, \beta \in B_n$. This is obtained by forming a diagram of $\alpha\beta\alpha^{-1}$ from three diagrams representing the three factors, pushing the upper diagram representing α along the n parallel strings on the right

so that eventually it comes to the diagram of α^{-1} from below. This gives $\widehat{\alpha\beta\alpha^{-1}} = \widehat{\beta\alpha\alpha^{-1}} = \widehat{\beta}$.

We prove the converse: any braids with isotopic closures in $V = D \times S^1$ are conjugate. To this end, we need to study closed braids in V in more detail. Set $\overline{V} = D \times \mathbf{R}$. Multiplying D by the universal covering

$$t \mapsto \exp(2\pi i t) : \mathbf{R} \to S^1 \,,$$

we obtain a universal covering $\overline{V} \to V$. Denote by T the covering transformation $\overline{V} \to \overline{V}$ sending (x,t) to $(x,t+1)$ for all $x \in D$, $t \in \mathbf{R}$.

If L is a closed n-braid in V, then its preimage $\overline{L} \subset \overline{V}$ is a 1-dimensional manifold meeting each disk $D \times \{t\}$ with $t \in \mathbf{R}$ transversely in n points. This implies that $\overline{L}$ consists of n components homeomorphic to $\mathbf{R}$. More information about $\overline{L}$ can be obtained by presenting L as the closure of a geometric braid $b \subset D \times I$, where we identify $I/\partial I = S^1$. Then

$$\overline{L} = \bigcup_{m \in \mathbf{Z}} T^m(b) \,.$$

By Section 1.7.2, $b = \bigcup_{t \in I} (f_t(Q), t)$ for a continuous family of homeomorphisms $\{f_t : D \to D\}_{t \in I}$ such that $f_0(Q) = Q$, $f_1 = \mathrm{id}_D$, and all f_t fix ∂D pointwise. We define a level-preserving self-homeomorphism of $\overline{V} = D \times \mathbf{R}$ by

$$(x,t) \mapsto (f_{t-[t]} f_0^{-[t]}(x), t) \,,$$

where $x \in D$, $t \in \mathbf{R}$, and $[t]$ is the greatest integer less than or equal to t. This homeomorphism fixes $\partial\overline{V} = \partial D \times \mathbf{R}$ pointwise and sends $Q \times \mathbf{R}$ onto $\overline{L}$; see Figure 2.6. The induced homeomorphism $(D - Q) \times \mathbf{R} \approx \overline{V} - \overline{L}$ shows that $D - Q = (D - Q) \times \{0\} \subset \overline{V} - \overline{L}$ is a deformation retract of $\overline{V} - \overline{L}$.

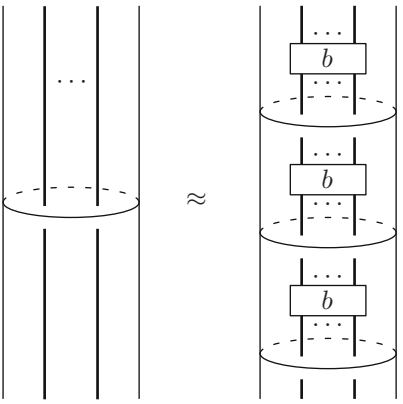

Fig. 2.6. A homeomorphism $(D \times \mathbf{R}, Q \times \mathbf{R}) \approx (D \times \mathbf{R}, \overline{L})$

Pick a point $d \in \partial D$ as in Figure 1.15 and set $\overline{d} = (d, 0) \in \overline{V}$. It is clear that the inclusion homomorphism $i : \pi_1(D-Q, d) \to \pi_1(\overline{V}-\overline{L}, \overline{d})$ is an isomorphism. By definition, $T(\overline{d}) = (d, 1)$. The covering transformation T restricted to $\overline{V} - \overline{L}$ induces an isomorphism $\pi_1(\overline{V} - \overline{L}, \overline{d}) \to \pi_1(\overline{V} - \overline{L}, T(\overline{d}))$. Consider the isomorphism $\pi_1(\overline{V} - \overline{L}, T(\overline{d})) \to \pi_1(\overline{V} - \overline{L}, \overline{d})$ obtained by conjugating the loops by the path $d \times [0, 1] \subset \partial D \times \mathbf{R} \subset \overline{V} - \overline{L}$. The composition $T_\#$ of these two isomorphisms is an automorphism of $\pi_1(\overline{V} - \overline{L}, \overline{d})$. It follows from the description of $\overline{L}$ given above that the following diagram is commutative:

$$\begin{array}{ccc} \pi_1(D - Q, d) & \xrightarrow{i} & \pi_1(\overline{V} - \overline{L}, \overline{d}) \\ {\scriptstyle \rho(f_0)}\downarrow & & \downarrow{\scriptstyle T_\#} \\ \pi_1(D - Q, d) & \xrightarrow{i} & \pi_1(\overline{V} - \overline{L}, \overline{d}) \end{array}$$

where $\rho(f_0)$ is the automorphism of $\pi_1(D - Q, d)$ induced by the restriction of f_0 to $D - Q$; cf. Section 1.6.3. Therefore $i^{-1}T_\# i = \rho(f_0)$. Indeed, the proof of Theorem 1.33 shows that the group homomorphism $\eta : B_n \to \mathfrak{M}(D, Q)$ introduced in Section 1.6.3 sends the braid $\beta \in B_n$ represented by b to the isotopy class of $f_0 : (D, Q) \to (D, Q)$. Identifying $\pi_1(D - Q, d)$ with the free group F_n on n generators $x_1, x_2, \ldots, x_n$ as in Section 1.6.3 and applying Theorem 1.33, we conclude that $\rho(f_0) = \rho\eta(\beta) = \widetilde{\beta}$ is the braid automorphism of F_n corresponding to β. Thus, $i^{-1}T_\# i = \widetilde{\beta}$.

Suppose now that $\beta, \beta' \in B_n$ are two braids with isotopic closures in V. Present them by geometric braids b, $b' \subset D \times I$ and let L, $L' \subset V$ be their respective closures. By assumption, there is a homeomorphism $g : V \to V$ such that g maps L onto L' preserving their canonical orientations and g is isotopic to the identity $\mathrm{id}_V : V \to V$. The latter condition implies that the restriction of g to ∂V is isotopic to the identity $\mathrm{id} : \partial V \to \partial V$. Therefore $g|_{\partial V}$ extends to a homeomorphism $g' : V \to V$ equal to the identity outside a narrow tubular neighborhood of ∂V in V. We can assume that this neighborhood is disjoint from L', so that g' is the identity on L'. Now, the homeomorphism $h = (g')^{-1}g : V \to V$ fixes ∂V pointwise and maps L onto L' preserving their canonical orientations. The former condition and the surjectivity of the inclusion homomorphism $\pi_1(\partial V) \to \pi_1(V) \cong \mathbf{Z}$ imply that h induces an identity automorphism of $\pi_1(V)$. Therefore h lifts to a homeomorphism $\overline{h} : \overline{V} \to \overline{V}$ such that $\overline{h}$ fixes $\partial\overline{V}$ pointwise, $\overline{h}T = T\overline{h}$, and $\overline{h}(\overline{L}) = \overline{L}'$. Hence $\overline{h}$ induces an isomorphism $\overline{h}_\# : \pi_1(\overline{V} - \overline{L}, \overline{d}) \to \pi_1(\overline{V} - \overline{L}', \overline{d})$ commuting with $T_\#$.

Consider the automorphism $\varphi = (i')^{-1}\overline{h}_\# i$ of $F_n = \pi_1(D - Q, d)$, where $i : \pi_1(D - Q, d) \to \pi_1(\overline{V} - \overline{L}, \overline{d})$ and $i' : \pi_1(D - Q, d) \to \pi_1(\overline{V} - \overline{L}', \overline{d})$ are the inclusion isomorphisms as above. We have $\widetilde{\beta}' = (i')^{-1}T_\# i'$ and

$$\varphi\widetilde{\beta}\varphi^{-1} = (i')^{-1}\overline{h}_\# i i^{-1}T_\# i i^{-1}(\overline{h}_\#)^{-1}i' = (i')^{-1}T_\# i' = \widetilde{\beta}' .$$

We claim that φ is a braid automorphism of F_n. This will imply that $\widetilde{\beta}$ and $\widetilde{\beta}'$ are conjugate in the group of braid automorphisms of F_n. By Theorem 1.31, this will imply that β and β' are conjugate in B_n.

By definition, the conjugacy classes of the generators

$$x_1, x_2, \dots, x_n \in F_n = \pi_1(D - Q, d)$$

are represented by small loops encircling the points of Q in D. The inclusion $D - Q = (D - Q) \times \{0\} \subset \overline{V} - \overline{L}$ maps these loops to small loops in $\overline{V} - \overline{L}$ encircling the components of $\overline{L}$. The homeomorphism $\overline{h} : \overline{V} \to \overline{V}$ transforms these loops into small loops in $\overline{V} - \overline{L}'$ encircling the components of $\overline{L}'$. The latter represent the conjugacy classes of the images of $x_1, x_2, \dots, x_n$ under the inclusion $D - Q = (D - Q) \times \{0\} \subset \overline{V} - \overline{L}'$. Hence φ transforms the conjugacy classes of $x_1, \dots, x_n$ into themselves, up to permutation. This verifies the first condition in the definition of a braid automorphism. The second condition says that $\varphi(x) = x$, where

$$x = x_1 x_2 \cdots x_n \in F_n = \pi_1(D - Q, d)\,.$$

Observe that x is represented by the loop ∂D based at d. The inclusion of $D - Q = (D - Q) \times \{0\}$ into $\overline{V} - \overline{L}$ maps this loop to $\partial D \times \{0\}$. Since $\overline{h}$ fixes $\partial \overline{V}$ pointwise, $\overline{h}_{\#} i(x) = i'(x)$ and therefore $\varphi(x) = x$. □

2.2.5 Closed braid diagrams

A *closed braid diagram* in the annulus $S^1 \times I$ is an oriented link diagram $\mathcal{D}$ in $S^1 \times I$ such that whenever a point moves along $\mathcal{D}$ in the positive direction, its projection to S^1 moves along S^1 counterclockwise without ever stopping or going backward. In other words, the projection $S^1 \times I \to S^1$ restricted to $\mathcal{D}$ is an orientation-preserving covering of S^1 (ramified at the crossings of $\mathcal{D}$). The number of points of $\mathcal{D}$ projecting to a given point on S^1 does not depend on the choice of that point, provided the crossings of $\mathcal{D}$ are counted with multiplicity 2. This number is called the *number of strands* of $\mathcal{D}$. Examples of closed braid diagrams on n strands in $S^1 \times I$ can be obtained by closing usual braid diagrams on n strands as in Figure 2.5.

Every closed braid diagram in $S^1 \times I$ presents a closed braid in the solid torus $S^1 \times I \times I$ in the obvious way; cf. Section 2.1.2. Clearly, every closed braid in $S^1 \times I \times I$ can be presented by a closed braid diagram in $S^1 \times I$.

We can apply to a closed braid diagram the moves $\Omega_2^{\mathrm{br}}, \Omega_3^{\mathrm{br}}$ and their inverses. These moves act as in Figures 1.5a and 1.5b, where the projections on the horizontal and vertical axes in the plane of the picture correspond to the projections to I and S^1, respectively. These moves keep the diagram in the class of closed braid diagrams and preserve the isotopy class of the closed braid represented by the diagram.

Lemma 2.2. *Two closed braid diagrams $\mathcal{D}$, $\mathcal{D}'$ in $S^1 \times I$ represent isotopic closed braids in the solid torus $S^1 \times I \times I$ if and only if $\mathcal{D}$ can be transformed into $\mathcal{D}'$ by a finite sequence of isotopies (in the class of closed braid diagrams) and moves $(\Omega_2^{\mathrm{br}})^{\pm 1}$, $(\Omega_3^{\mathrm{br}})^{\pm 1}$.*

Proof. We need only prove that if $\mathcal{D}, \mathcal{D}'$ represent isotopic closed braids in the solid torus, then $\mathcal{D}$ can be transformed into $\mathcal{D}'$ by a finite sequence of isotopies and moves $(\Omega_2^{\rm br})^{\pm 1}, (\Omega_3^{\rm br})^{\pm 1}$. Pick a point $z \in S^1$ such that the interval $\{z\} \times I$ does not meet the crossings of $\mathcal{D}$ or $\mathcal{D}'$. Cutting open $\mathcal{D}, \mathcal{D}'$ along this interval, we obtain two braid diagrams b, b', respectively. By Theorem 2.1, they represent conjugate braids. Applying a $\Omega_2^{\rm br}$-move to $\mathcal{D}$ in a neighborhood of $\{z\} \times I$, we can transform b into $\sigma_i b \sigma_i^{-1}$ and $\sigma_i^{-1} b \sigma_i$ for any $i = 1, 2, \ldots, n-1$. Applying such moves recursively, we can transform b into an arbitrary conjugate diagram. Thus we can assume that b and b' represent isotopic braids. Then, by Theorem 1.6, these diagrams can be related by a finite sequence of isotopies and braidlike moves. This induces a sequence of isotopies and braidlike moves transforming $\mathcal{D}$ into $\mathcal{D}'$. □

Exercise 2.2.1. Verify that for any $\beta \in B_n$, the number of components of the closed braid $\widehat{\beta}$ is equal to the number of cycles in the decomposition of the permutation $\pi(\beta) \in \mathfrak{S}_n$ as a product of commuting cycles.

Exercise 2.2.2. The closure of a pure braid $\beta \in P_n$ is an ordered n-component link: its ith component is the closure of the ith string of β for $i = 1, 2, \ldots, n$. Prove that for any $\beta, \beta' \in P_n$, the links $\widehat{\beta}, \widehat{\beta}'$ are isotopic in the solid torus in the class of ordered oriented links if and only if β and β' are conjugate in P_n.

Exercise 2.2.3. Prove that if two closed braids L, $L' \subset V = D \times S^1$ are isotopic, then they are isotopic in the class of closed braids in V, that is, there is an isotopy $\{F_s : V \to V\}_{s \in I}$ of L into L' such that $F_s(L)$ is a closed braid for all $s \in I$. (Hint: Use Theorem 2.1.)

Exercise 2.2.4. Let $L \subset V$ be a closed braid. Prove that the kernel of the inclusion homomorphism $\pi_1(V - L) \to \pi_1(V) = \mathbf{Z}$ is a free group. (Hint: In the notation of Section 2.2.4, this kernel is isomorphic to $\pi_1(\overline{V} - \overline{L}, \overline{d})$.)

2.3 Alexander's theorem

We establish here a fundamental theorem, due to J. W. Alexander, asserting that all links in $\mathbf{R}^3$ are isotopic to closed braids.

2.3.1 Closed braids in $\mathbf{R}^3$

Pick a Euclidean circle in the plane $\mathbf{R}^2 \times \{0\} \subset \mathbf{R}^3$ with center at the origin $O = (0, 0, 0)$. We identify a closed cylindrical neighborhood of this circle in $\mathbf{R}^3$ with the solid torus $V = D \times S^1$. By a *closed n-braid in* $\mathbf{R}^3$, we shall mean an oriented geometric link in $\mathbf{R}^3$ lying in $V \subset \mathbf{R}^3$ as a closed n-braid with its canonical counterclockwise orientation (cf. Figure 2.3, where the plane $\mathbf{R}^2 \times \{0\}$ is the plane of the picture).

In particular, for any $\beta \in B_n$, the closed braid $\widehat{\beta} \subset V$ yields a closed braid in $\mathbf{R}^3$ via the inclusion $V \subset \mathbf{R}^3$; cf. Figure 2.4. The latter closed braid is also denoted by $\widehat{\beta}$ and is called the *closure* of β. A diagram of $\widehat{\beta}$ is obtained from a diagram of β by connecting the bottom endpoints with the top endpoints by n standard arcs; cf. Figure 2.5, where the dotted circles should be disregarded. We stress that closed braids in $\mathbf{R}^3$ are *oriented* geometric links.

For example, the closure of the trivial braid on n strings is a trivial n-component link. The closure of $\sigma_1^{\pm 1} \in B_2$ is a trivial knot. The closure of $\sigma_1^{\pm 2} \in B_2$ is an oriented Hopf link. More generally, the closure of $\sigma_1^m \in B_2$ with $m \in \mathbf{Z}$ is a so-called *torus* $(2, m)$*-link*. It has two components for even m and one component for odd m.

We can give an equivalent but more direct definition of closed braids in $\mathbf{R}^3$. Consider the coordinate axis $\ell = \{(0,0)\} \times \mathbf{R} \subset \mathbf{R}^3$ meeting the plane $\mathbf{R}^2 \times \{0\}$ at the origin $O = (0,0,0)$. The counterclockwise rotation about O in the plane $\mathbf{R}^2 \times \{0\}$ determines a positive direction of rotation about ℓ. An oriented geometric link $L \subset \mathbf{R}^3 - \ell$ is a *closed* n*-braid* if the vector from O to any point $X \in L$ rotates in the positive direction about ℓ when X moves along L in the direction determined by the orientation of L. The equivalence of this definition with the previous one can be seen as follows. Pick a Euclidean disk D lying in an open half-plane bounded by ℓ in $\mathbf{R}^3$ and having its center in $\mathbf{R}^2 \times \{0\}$. Rotating D around ℓ, we sweep a solid torus $V = D \times S^1$ as above. Taking D big enough, we can assume that a given link $L \subset \mathbf{R}^3 - \ell$ lies in V. It is clear that L is a closed braid in the sense of the first definition if and only if L is a closed braid in the sense of the second definition.

Theorem 2.3 (J. W. Alexander). *Any oriented link in* $\mathbf{R}^3$ *is isotopic to a closed braid.*

Proof. By a *polygonal link*, we shall mean a geometric link in $\mathbf{R}^3$ whose components are closed broken lines. By *vertices* and *edges* of a polygonal link, we mean the vertices and the edges of its components. It is well known that any geometric link in $\mathbf{R}^3$ is isotopic to a polygonal link (cf. the proof of Theorem 1.6). We need only to prove that any oriented polygonal link $L \subset \mathbf{R}^3$ is isotopic to a closed braid. Moving slightly the vertices of L in $\mathbf{R}^3$, we obtain a polygonal link isotopic to L. We use such small deformations to ensure that $L \subset \mathbf{R}^3 - \ell$ and that the edges of L do not lie in planes containing the axis $\ell = \{(0,0)\} \times \mathbf{R}$. Let

$$AC \subset L \subset \mathbf{R}^3 - \ell$$

be an edge of L, where L is oriented from A to C. The edge AC is said to be *positive* (resp. *negative*) if the vector from the origin $O \in \ell$ to a point $X \in AC$ rotates in the positive (resp. negative) direction about ℓ when X moves from A to C. The assumption that AC does not lie in a plane containing ℓ implies that AC is necessarily positive or negative. The edge AC of L is said to be *accessible* if there is a point $B \in \ell$ such that the triangle ABC meets L only along AC.

If all edges of L are positive, then L is a closed braid and there is nothing to prove. Consider a negative edge AC of L. We replace AC with a sequence of positive edges as follows. If AC is accessible, then we pick $B \in \ell$ such that the triangle ABC meets L only along AC. In the plane ABC we take a slightly bigger triangle $AB'C$ containing B in its interior, meeting ℓ only at B, and meeting L only along AC; see Figure 2.7. We apply to L the Δ-*move* $\Delta(AB'C)$ replacing AC with two positive edges AB' and $B'C$ (see Section 1.2.3 for similar moves on geometric braids; in contrast to the setting of braids, we impose here no conditions on the third coordinates of the vertices). The resulting polygonal link is isotopic to L and has one negative edge fewer than L.

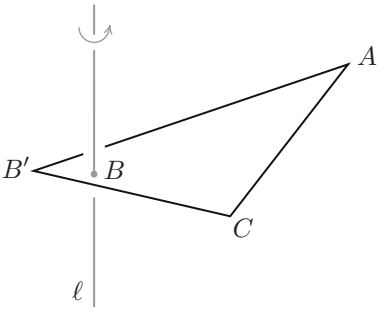

Fig. 2.7. The triangle $AB'C$

Suppose that the edge AC is not accessible. Note that every point P of AC is contained in an accessible subsegment of AC. (To see this, pick $B \in \ell$ such that the segment PB meets L only at P and then slightly "thicken" this segment inside the triangle ABC to obtain a triangle P^-BP^+ meeting L along its side $P^-P^+ \subset AC$ containing P. Then P^-P^+ is an accessible subsegment of AC.) Since AC is compact, we can split it into a finite number of consecutive accessible subsegments. We apply to each of them the Δ-move as above choosing the corresponding points $B \in \ell$ distinct and choosing B' close enough to B to stay away from other edges of L. Since AC does not lie in a plane containing ℓ, the triangles determining these Δ-moves meet only at the common vertices of the consecutive subsegments of AC (to see this, consider the projections of these segments and triangles to the plane $\{0\} \times \mathbf{R}^2$ orthogonal to ℓ). Therefore these Δ-moves do not hinder each other and may be performed in an arbitrary order. They replace $AC \subset L$ with a finite sequence of positive edges, beginning at A and ending at C. The resulting polygonal link is isotopic to L in $\mathbf{R}^3$. Applying this procedure inductively to all negative edges of L, we obtain a closed braid isotopic to L. □

Exercise 2.3.1. Verify that the oriented 2-component links obtained by closing $\sigma_1^2 \in B_2$ and $\sigma_1^{-2} \in B_2$ are not isotopic, while the underlying unoriented links are isotopic. (Hint: Consider the linking number of the components.)

Exercise 2.3.2. Observe that the closure of σ_1^3 is the trefoil knot shown on the left of Figure 2.1 and endowed with an orientation. Observe that the closure of $\sigma_1^{-1}\sigma_2\sigma_1^{-1}\sigma_2$ is the figure-eight knot shown in Figure 2.1 and endowed with an orientation.

Exercise 2.3.3. Verify that the oriented link in $\mathbf{R}^3$ obtained by inverting the orientation of all components of the closure of a braid $\sigma_{i_1}^{r_1}\sigma_{i_2}^{r_2}\cdots\sigma_{i_m}^{r_m}$, where $r_1, r_2, \ldots, r_m \in \mathbf{Z}$, is isotopic to the closure of $\sigma_{i_m}^{r_m}\cdots\sigma_{i_2}^{r_2}\sigma_{i_1}^{r_1}$.

2.4 Links as closures of braids: an algorithm

By Alexander's theorem, every oriented link $L \subset \mathbf{R}^3$ is isotopic to a closed braid. It is useful to be able to find such a braid starting from a diagram of L. The proof of Alexander's theorem given above is not of much help: in the course of the proof, the diagram is modified by global transformations over which we have little control. In this section we give a simple algorithm deriving from any diagram of L a braid whose closure is isotopic to L. Incidentally, this will give another proof of Alexander's theorem.

2.4.1 Preliminaries

We observe first that any two disjoint oriented (topological) circles on the sphere S^2 bound an annulus in S^2. These circles are said to be *incompatible* if their orientation is induced by an orientation of this annulus. Otherwise, these circles are *compatible*. For instance, two oriented concentric cirles in $\mathbf{R}^2 \subset S^2$ are compatible if they both are oriented clockwise or both counterclockwise.

Consider an oriented link diagram $\mathcal{D}$ in $\mathbf{R}^2$. Near each crossing point x of $\mathcal{D}$ the diagram looks either like the 2-braid σ_1 or like the 2-braid σ_1^{-1}. A *smoothing* of $\mathcal{D}$ at x replaces this 2-braid with a trivial 2-braid and keeps the rest of $\mathcal{D}$ untouched; see Figure 2.8. Smoothing $\mathcal{D}$ at all crossings, we obtain a closed oriented 1-dimensional submanifold of $\mathbf{R}^2$. It consists of a finite number of disjoint oriented (topological) circles called the *Seifert circles* of $\mathcal{D}$. The number of Seifert circles of $\mathcal{D}$ is denoted by $n(\mathcal{D})$. Two Seifert circles of $\mathcal{D}$ are *compatible* (resp. *incompatible*) if they are compatible (resp. incompatible) in $S^2 = \mathbf{R}^2 \cup \{\infty\}$. The number of pairs of incompatible Seifert circles of $\mathcal{D}$ is denoted by $h(\mathcal{D})$ and is called the *height* of $\mathcal{D}$. Clearly, $0 \leq h(\mathcal{D}) \leq n(n-1)/2$, where $n = n(\mathcal{D})$. Both numbers $n(\mathcal{D})$ and $h(\mathcal{D})$ are isotopy invariants of $\mathcal{D}$.

An oriented link diagram $\mathcal{D}$ in $\mathbf{R}^2$ is a *closed braid diagram on n strands* if it lies in an annulus $S^1 \times I \in \mathbf{R}^2$ and is a closed braid diagram in this annulus in the sense of Section 2.2.5. It is understood that all strands of $\mathcal{D}$ are oriented counterclockwise.

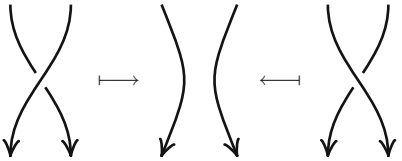

Fig. 2.8. Smoothing of a crossing

Examples of such $\mathcal{D}$ are obtained from braid diagrams on n strands by connecting the bottom and top endpoints by n disjoint arcs in $\mathbf{R}^2$ as in Figure 2.5, with orientation of the strands induced by the orientation on the braid from the top to the bottom. Smoothing a closed braid diagram $\mathcal{D}$ on n strands at all crossings, we obtain a closed braid diagram on n strands without crossings. Such a diagram consists of n disjoint concentric circles in $\mathbf{R}^2$ with counterclockwise orientation. Thus, $n(\mathcal{D}) = n$ and $h(\mathcal{D}) = 0$.

2.4.2 Bending and tightening of link diagrams

Consider an oriented link diagram $\mathcal{D}$ in $\mathbf{R}^2$. Let

$$|\mathcal{D}| \subset \mathbf{R}^2$$

be the union of the components of $\mathcal{D}$ with the over/undercrossing data forgotten. This is a 4-valent graph in $\mathbf{R}^2$ whose vertices are the crossings of $\mathcal{D}$. By an *edge* of $\mathcal{D}$, we mean a connected component of the complement of the set of crossings in $|\mathcal{D}|$. Edges of $\mathcal{D}$ are embedded arcs or circles in $\mathbf{R}^2$ (the circles arise from the components of $\mathcal{D}$ having no crossings). By a *face* of $\mathcal{D}$, we mean a connected component of $\mathbf{R}^2 - |\mathcal{D}|$. We say that a face f of $\mathcal{D}$ is *adjacent* to an edge a of $\mathcal{D}$ if a is contained in the closure of f. We say that f is *adjacent* to a Seifert circle S of $\mathcal{D}$ if f is adjacent to at least one edge of $\mathcal{D}$ contained in S. A face f of $\mathcal{D}$ is a *defect face* if f is adjacent to distinct edges a_1, a_2 of $\mathcal{D}$ such that the Seifert circles S_1, S_2 of $\mathcal{D}$ going along a_1, a_2 are distinct and incompatible. An oriented embedded arc $c \subset \mathbf{R}^2$ leading from a point of a_1 to a point of a_2 and lying (except the endpoints) in f is called a *reduction arc* of $\mathcal{D}$ in f. The incompatibility of S_1, S_2 may be reformulated by saying that one of the edges a_1, a_2 crosses c from right to left and the other one crosses c from left to right. Given such a_1, a_2, c, we can apply to $\mathcal{D}$ the second Reidemeister move pushing a subarc of a_1 along c and then sliding it over a_2; see Figure 2.9. We call this move a *bending* of $\mathcal{D}$ along c *involving the (incompatible) Seifert circles* S_1, S_2. This move produces a diagram of an isotopic link. The inverse move is called a *tightening*.

For example, consider the diagram $\mathcal{D}$ of a trivial knot in $\mathbf{R}^3$ shown on the left of Figure 2.10. The underlying graph $|\mathcal{D}|$ has two vertices and four edges. Smoothing $\mathcal{D}$ at both crossings, we obtain three Seifert circles. All three are oriented counterclockwise and one of them encloses the other two.

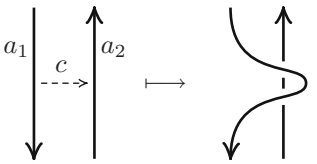

Fig. 2.9. Bending along an arc c

The two smaller circles are incompatible with each other and compatible with the bigger circle. Thus, $n(\mathcal{D}) = 3$ and $h(\mathcal{D}) = 1$. The diagram $\mathcal{D}$ has one defect face. A reduction arc in this face is represented by the dotted arrow on the left-hand side of Figure 2.10. Bending $\mathcal{D}$ along this arc, we obtain the diagram on the right-hand side of Figure 2.10. This diagram is a closed braid diagram in the annulus bounded by the dotted circles. (This diagram is isotopic to the closure of $\sigma_1\sigma_2\sigma_1\sigma_2^{-1}$.) As we shall see below, this example is typical in the sense that any oriented link diagram can be transformed by a sequence of bendings and isotopies into a closed braid diagram.

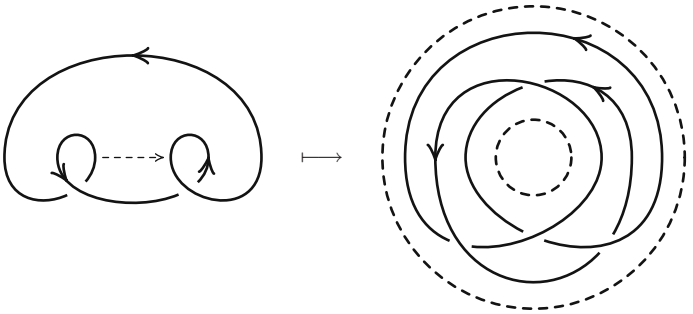

Fig. 2.10. Example of a bending

The following three lemmas give a key to the transformation of link diagrams into closed braid diagrams.

Lemma 2.4. *If $\mathcal{D}'$ is obtained from an oriented link diagram $\mathcal{D}$ in $\mathbf{R}^2$ by a bending, then $n(\mathcal{D}') = n(\mathcal{D})$ and $h(\mathcal{D}') = h(\mathcal{D}) - 1$.*

Proof. Let S_1, S_2 be the incompatible (distinct) Seifert circles of $\mathcal{D}$ involved in the bending; see Figure 2.11. The small biangle created by the bending gives rise to a Seifert circle of $\mathcal{D}'$, denoted by S_0. The remaining parts of S_1, S_2 give rise to a Seifert circle of $\mathcal{D}'$, denoted by S_∞. All other Seifert circles of $\mathcal{D}$ survive in $\mathcal{D}'$ without changes. Therefore $n(\mathcal{D}') = n(\mathcal{D})$. Note that the Seifert circles of $\mathcal{D}$ and $\mathcal{D}'$ do not pass through the shaded areas in Figure 2.11.

We now compare the heights $h(\mathcal{D})$ and $h(\mathcal{D}')$. Observe first that the Seifert circles S_1, S_2 bound respective disjoint disks D_1, D_2 in $S^2 = \mathbf{R}^2 \cup \{\infty\}$.

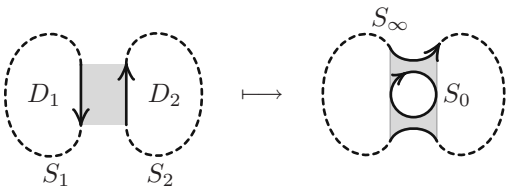

Fig. 2.11. Seifert circles before and after bending

For $i = 1, 2$, let d_i denote the number of Seifert circles of $\mathcal{D}$ lying in the open disk $D_i^\circ = D_i - \partial D_i$. Let d be the number of Seifert circles of $\mathcal{D}$ lying in the annulus $S^2 - (D_1 \cup D_2)$ and incompatible with S_1. Finally, let h be the number of pairs of incompatible Seifert circles of $\mathcal{D}$ both distinct from S_1, S_2. We claim that

$$h(\mathcal{D}) = h + d_1 + d_2 + 2d + 1\,.$$

It suffices to verify that the number of pairs of incompatible Seifert circles of $\mathcal{D}$ including S_1 or S_2 or both is equal to $d_1 + d_2 + 2d + 1$. For $i = 1, 2$, an oriented circle in D_i° is incompatible with S_1 or S_2, but not with both. This gives the contribution $d_1 + d_2$. An oriented circle in $S^2 - (D_1 \cup D_2)$ is incompatible with S_1 if and only if it is incompatible with S_2. This contributes $2d$. Finally, S_1 and S_2 are incompatible, which contributes 1.

We claim that

$$h(\mathcal{D}') = h + d_1 + d_2 + 2d = h(\mathcal{D}) - 1\,.$$

It suffices to verify that the number of pairs of incompatible Seifert circles of $\mathcal{D}'$ including S_0 or S_∞ or both is equal to $d_1 + d_2 + 2d$. For $i = 1, 2$, an oriented circle in D_i° is always incompatible with S_0 or S_∞, but not with both. This contributes $d_1 + d_2$. An oriented circle in $S^2 - (D_1 \cup D_2)$ is incompatible with S_0 if and only if it is incompatible with S_∞ and if and only if it is incompatible with S_1. This contributes $2d$. Finally, S_0 and S_∞ are compatible. Hence $h(\mathcal{D}') = h(\mathcal{D}) - 1$. □

Lemma 2.5. *An oriented link diagram $\mathcal{D}$ in $\mathbf{R}^2$ has a defect face if and only if $h(\mathcal{D}) \neq 0$.*

Proof. Cutting S^2 open along the Seifert circles of $\mathcal{D}$, we obtain a compact surface Σ with boundary. For a crossing x of $\mathcal{D}$, denote by γ_x a line segment near x joining the Seifert circles as in Figure 2.12. These segments are all disjoint and each of them lies in a component of Σ.

If $\mathcal{D}$ has a defect face, then clearly $h(\mathcal{D}) > 0$. We prove the converse: if $h(\mathcal{D}) > 0$, then $\mathcal{D}$ has a defect face. We first prove that there are a component F of Σ and two Seifert circles in ∂F whose orientation is induced by an orientation on F. Pick two incompatible Seifert circles S_1, S_2 of $\mathcal{D}$ and consider an oriented embedded arc $c \subset \mathbf{R}^2$ leading from a point of S_1 to a point of S_2. We can assume that c meets each Seifert circle of $\mathcal{D}$ transversely in at

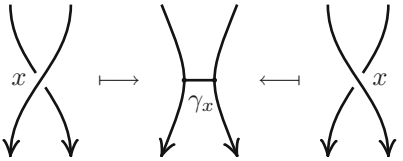

Fig. 2.12. The segment γ_x

most one point. The crossings of c with these circles form a finite subset of c including the endpoints. At each of the crossings, the corresponding Seifert circle is directed to the left or to the right of c. The incompatibility of S_1, S_2 means that their directions at the endpoints of c are opposite: one of these circles is directed to the left of c and the other one is directed to the right of c. Therefore, among the crossings of c with the Seifert circles of $\mathcal{D}$, there are two that lie *consecutively* on c and at which the directions of the corresponding Seifert circles are opposite. The component F of Σ containing the subarc of c between two such crossings satisfies the requirements above. Warning: this subarc may meet certain segments γ_x; then it does not lie in a face of $\mathcal{D}$.

Consider in more detail a component F of Σ such that there are at least two Seifert circles in ∂F whose orientation is induced by an orientation on F. Fix such an orientation on F. Let us call a Seifert circle in ∂F *positive* if its orientation is induced by the one on F and *negative* otherwise. By assumption, there are at least two positive Seifert circles in ∂F. If F contains no segments γ_x, then $F^\circ = F - \partial F$ is a face of $\mathcal{D}$ adjacent to ≥ 2 positive Seifert circles in ∂F. Hence this face is a defect face. Suppose that F contains certain segments γ_x. Removing them all from F, we obtain a subsurface $F' \subset F$. It is clear that any component f of F' is adjacent to at least one segment γ_x and the interior of f is a face of $\mathcal{D}$. Each $\gamma_x \subset F$ connects a positive Seifert circle in ∂F with a negative one. Therefore f is adjacent to at least one positive and at least one negative Seifert circle. If f is adjacent to at least two positive or to at least two negative Seifert circles, then f is a defect face. Suppose that each component f of F' is adjacent to exactly one positive and exactly one negative Seifert circle. Note that moving from f to a neighboring component of F' across some $\gamma_x \subset F$, we meet the same Seifert circles. Since F is connected, we can move in this way from any component of F' to any other component. Therefore ∂F contains exactly one positive and one negative Seifert circle. This contradicts our assumptions. Hence $\mathcal{D}$ has a defect face. □

Lemma 2.6. *An oriented link diagram $\mathcal{D}$ in $\mathbf{R}^2$ with $h(\mathcal{D}) = 0$ is isotopic in the sphere $S^2 = \mathbf{R}^2 \cup \{\infty\}$ to a closed braid diagram in $\mathbf{R}^2$.*

Proof. Let Σ and $\{\gamma_x\}_x$ be the same objects as in the proof of the previous lemma. Suppose that $h(\mathcal{D}) = 0$. We must prove that $\mathcal{D}$ is isotopic in S^2 to a closed braid diagram in the plane $\mathbf{R}^2 = S^2 - \{\infty\}$. If a certain component of the surface Σ has three or more boundary components, then two of them must be incompatible in S^2, which contradicts our assumption $h(\mathcal{D}) = 0$.

A compact connected subsurface of the 2-sphere whose boundary has one or two components is a disk or an annulus. Thus, Σ consists only of disks and annuli. An induction on the number of annuli components of Σ shows that the Seifert circles of $\mathcal{D}$ can be transformed by an isotopy of S^2 into a union of disjoint concentric circles in $\mathbf{R}^2$. Applying this isotopy of S^2 to $\mathcal{D}$, we can assume from the very beginning that the Seifert circles of $\mathcal{D}$ are concentric circles in $\mathbf{R}^2$. The equality $h(\mathcal{D}) = 0$ implies that all these circles are oriented in the same direction, either clockwise or counterclockwise. In the first case we apply to $\mathcal{D}$ an additional isotopy pushing all its Seifert circles across $\infty \in S^2$ so that in the final position the Seifert circles of $\mathcal{D}$ become concentric circles in $\mathbf{R}^2$ with counterclockwise orientation. With a further isotopy of $\mathcal{D}$, we can additionally ensure that these circles are concentric Euclidean circles and the segments γ_x are radial, i.e., are contained in some radii. The resulting link diagram is transversal to all radii and therefore is a closed braid diagram. □

2.4.3 The algorithm

Now we can describe an algorithm transforming any diagram $\mathcal{D}$ of an oriented link L in $\mathbf{R}^3$ into a closed braid diagram of L. It suffices to perform a bending on the diagram each time there is a defect face. By Lemmas 2.4 and 2.5, this process stops after $h(\mathcal{D})$ steps and yields a diagram $\mathcal{D}'$ of L with $n(\mathcal{D}') = n(\mathcal{D})$ and $h(\mathcal{D}') = 0$. By Lemma 2.6, $\mathcal{D}'$ is isotopic in S^2 to a closed braid diagram, $\mathcal{D}_0$, in $\mathbf{R}^2$. The latter diagram also represents L; cf. Exercise 2.1.2. Since the number of Seifert circles is an isotopy invariant, $n(\mathcal{D}_0) = n(\mathcal{D}') = n(\mathcal{D})$. Thus $\mathcal{D}_0$ is a closed braid diagram on $n = n(\mathcal{D})$ strands. If $\mathcal{D}$ has k crossings, then $\mathcal{D}_0$ has $k + 2h(\mathcal{D})$ crossings. The corresponding braid is represented by a word of length $k + 2h(\mathcal{D}) \leq k + n(n-1)$ in the generators $\sigma_1^{\pm 1}, \ldots, \sigma_{n-1}^{\pm 1} \in B_n$.

Note the following corollary of this algorithm.

Corollary 2.7. *If an oriented link in $\mathbf{R}^3$ is presented by a diagram with n Seifert circles, then it is isotopic to a closed n-braid.*

The converse to this corollary is also true, since as we know, a closed braid diagram on n strands has n Seifert circles.

Exercise 2.4.1. Show that smoothing of a crossing (or of any number of crossings) on an oriented link diagram does not increase the number of defect faces.

Solution. Let $\mathcal{D}$ be an oriented link diagram and let $\mathcal{D}_x$ be the oriented link diagram obtained from $\mathcal{D}$ by smoothing at a crossing x. Observe that $\mathcal{D}$ and $\mathcal{D}_x$ have the same Seifert circles. Denote by γ_x the line segment near x joining Seifert circles as in Figure 2.12. Let f be the face of $\mathcal{D}_x$ containing γ_x. If $f - \gamma_x$ is connected, then $\mathcal{D}$ and $\mathcal{D}_x$ have the same faces. Then they have an equal number of defect faces. Suppose that γ_x splits f into two connected pieces f_1, f_2, which are then faces of $\mathcal{D}$. It suffices to prove that if f_1, f_2 are

not defect faces of $\mathcal{D}$, then f is not a defect face of $\mathcal{D}_x$. Since f_1 (resp. f_2) is not a defect face, it is adjacent to at most two Seifert circles. Since $\gamma_x \subset f$ joins Seifert circles of different signs (with respect to any orientation of f), these circles are distinct and compatible. Therefore f_1 and f_2 are adjacent to the same pair of distinct compatible Seifert circles. The face f is adjacent to the same circles. Therefore f is not a defect face.

2.5 Markov's theorem

We state a fundamental theorem that allows us to describe all braids with isotopic closures in $\mathbf{R}^3$. This theorem, due to A. Markov, is based on so-called Markov moves on braids.

2.5.1 Markov moves

The presentation of an oriented link in $\mathbf{R}^3$ as a closed braid is far from being unique. As we know, if two braids $\beta, \beta' \in B_n$ are conjugate (we record it as $\beta \sim_c \beta'$), then their closures $\widehat{\beta}$, $\widehat{\beta'}$ are isotopic in the solid torus and a fortiori in $\mathbf{R}^3$. In general, the converse is not true. For instance, the closures of the 2-string braids σ_1, σ_1^{-1} are trivial knots although these braids are not conjugate in $B_2 \cong \mathbf{Z}$. There is another simple construction of braids with isotopic closures. For $\beta \in B_n$, consider the braids $\sigma_n\, \iota(\beta)$ and $\sigma_n^{-1}\iota(\beta)$, where ι is the natural embedding $B_n \hookrightarrow B_{n+1}$. Drawing pictures, one easily observes that the closures of $\sigma_n\, \iota(\beta)$ and $\sigma_n^{-1}\iota(\beta)$ are isotopic to $\widehat{\beta}$ in $\mathbf{R}^3$.

For $\beta, \gamma \in B_n$, the transformation $\beta \mapsto \gamma\beta\gamma^{-1}$ is called the *first Markov move* and is denoted by M_1. The transformation $\beta \mapsto \sigma_n^{\varepsilon}\, \iota(\beta)$ with $\varepsilon = \pm 1$ is called the *second Markov move* and is denoted by M_2. Note that the inverse to an M_1-move is again an M_1-move. We shall say that two braids β, β' (possibly with different numbers of strings) are M-*equivalent* if they can be related by a finite sequence of moves $\mathrm{M}_1, \mathrm{M}_2, \mathrm{M}_2^{-1}$, where M_2^{-1} is the inverse of an M_2-move. We record it as $\beta \sim \beta'$. It is clear that the M-equivalence $\sim$ is an equivalence relation on the disjoint union $\amalg_{n\geq 1} B_n$ of all braid groups. For example, the braids $\sigma_1, \sigma_1^{-1} \in B_2$ are M-equivalent. Indeed, using the equalities $\sigma_2^{-1}\sigma_1^{-1}\sigma_2^{-1} = \sigma_1^{-1}\sigma_2^{-1}\sigma_1^{-1}$ and $\sigma_1^{-1}\sigma_2^{-1}\sigma_1 = \sigma_2\sigma_1^{-1}\sigma_2^{-1}$, we obtain

$$\begin{aligned}
\sigma_1 &\sim \sigma_2^{-1}\sigma_1 \sim_c (\sigma_1\sigma_2)^{-1}(\sigma_2^{-1}\sigma_1)(\sigma_1\sigma_2) \\
&= \sigma_2^{-1}\sigma_1^{-1}\sigma_2^{-1}\sigma_1^2\sigma_2 = \sigma_1^{-1}\sigma_2^{-1}\sigma_1^{-1}\sigma_1^2\sigma_2 \\
&= \sigma_1^{-1}\sigma_2^{-1}\sigma_1\sigma_2 = \sigma_2\sigma_1^{-1}\sigma_2^{-1}\sigma_2 \\
&= \sigma_2\sigma_1^{-1} \sim \sigma_1^{-1}\,.
\end{aligned}$$

As we saw, the closures of M-equivalent braids are isotopic as oriented links in $\mathbf{R}^3$. The following deep theorem asserts that conversely, any two braids with isotopic closures are M-equivalent.

Theorem 2.8 (A. Markov). *Two braids (possibly with different numbers of strings) have isotopic closures in Euclidean space* $\mathbf{R}^3$ *if and only if these braids are M-equivalent.*

The following fundamental corollary yields a description of the set of isotopy classes of oriented links in $\mathbf{R}^3$ in terms of braids.

Corollary 2.9. *Let* $\mathcal{L}$ *be the set of all isotopy classes of nonempty oriented links in* $\mathbf{R}^3$*. The mapping* $\amalg_{n\geq 1} B_n \to \mathcal{L}$ *assigning to a braid the isotopy class of its closure induces a bijection from the quotient set* $(\amalg_{n\geq 1} B_n)/\sim$ *onto* $\mathcal{L}$*.*

Here the surjectivity follows from Alexander's theorem, while the injectivity follows from Markov's theorem.

The proof of Theorem 2.8 starts in Section 2.5.3 and occupies the rest of the chapter.

2.5.2 Markov functions

Corollary 2.9 allows one to identify isotopy invariants of oriented links in $\mathbf{R}^3$ with functions on $\amalg_{n\geq 1} B_n$ constant on the M-equivalence classes. This leads us to the following definition.

Definition 2.10. *A Markov function with values in a set* E *is a sequence of set-theoretic maps* $\{f_n : B_n \to E\}_{n\geq 1}$*, satisfying the following conditions:*

(i) for all $n \geq 1$ *and all* $\alpha, \beta \in B_n$*,*

$$f_n(\alpha\beta) = f_n(\beta\alpha)\,; \tag{2.1}$$

(ii) for all $n \geq 1$ *and all* $\beta \in B_n$*,*

$$f_n(\beta) = f_{n+1}(\sigma_n\beta) \quad \textit{and} \quad f_n(\beta) = f_{n+1}(\sigma_n^{-1}\beta)\,. \tag{2.2}$$

For example, for any $e \in E$, the constant maps $B_n \to E$ sending B_n to e for all n form a Markov function. More interesting examples of Markov functions will be given in Chapters 3 and 4.

Any Markov function $\{f_n : B_n \to E\}_{n\geq 1}$ determines an E-valued isotopy invariant $\widehat{f}$ of oriented links in $\mathbf{R}^3$ as follows. Let L be an oriented link in $\mathbf{R}^3$. Pick a braid $\beta \in B_n$ whose closure is isotopic to L and set $\widehat{f}(L) = f_n(\beta) \in E$. Note that $\widehat{f}(L)$ does not depend on the choice of β. Indeed, if $\beta' \in B_{n'}$ is another braid whose closure is isotopic to L, then β and β' are M-equivalent (Theorem 2.8). It follows directly from the definition of M-equivalence and the definition of a Markov function that $f_n(\beta) = f_{n'}(\beta')$. The function $\widehat{f}$ is an isotopy invariant of oriented links: if L, L' are isotopic oriented links in $\mathbf{R}^3$ and $\beta \in B_n$ is a braid whose closure is isotopic to L, then the closure of β is also isotopic to L' and $\widehat{f}(L) = f_n(\beta) = \widehat{f}(L')$.

2.5.3 A pivotal lemma

We formulate an important lemma needed in the proof of Theorem 2.8. We begin with some notation. Given two braids $\alpha \in B_m$ and $\beta \in B_n$, we form their *tensor product* $\alpha \otimes \beta \in B_{m+n}$ by placing β to the right of α without any mutual intersection or linking; see Figure 2.13. Here the vertical lines represent bunches of parallel strands with the number of strands indicated near the line.

A diagram of $\alpha \otimes \beta$ is obtained by placing a diagram of β to the right of a diagram of α without mutual crossings. For example, $1_m \otimes 1_n = 1_{m+n}$, where 1_m is the trivial braid on m strands. Clearly,

$$\alpha \otimes \beta = (\alpha \otimes 1_n)(1_m \otimes \beta) = (1_m \otimes \beta)(\alpha \otimes 1_n)\,.$$

Note also that

$$(\alpha \otimes \beta) \otimes \gamma = \alpha \otimes (\beta \otimes \gamma)$$

for any braids α, β, γ. This allows us to suppress the parentheses and to write simply $\alpha \otimes \beta \otimes \gamma$.

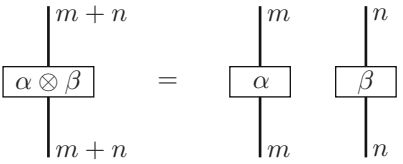

Fig. 2.13. The tensor product of braids

For a sign $\varepsilon = \pm$ and any integers $m, n \geq 0$ with $m + n \geq 1$, we define a braid $\sigma^{\varepsilon}_{m,n} \in B_{m+n}$ as follows. Consider the standard diagram of $\sigma_1 \in B_2$ consisting of two strands with one crossing. Replacing the overcrossing strand with m parallel strands running very closely to each other and similarly replacing the undercrossing strand with n parallel strands, we obtain a braid diagram with $m + n$ strands and mn crossings. This diagram represents $\sigma^{+}_{m,n} \in B_{m+n}$. Transforming all overcrossings in the latter diagram into undercrossings, we obtain a diagram of $\sigma^{-}_{m,n} \in B_{m+n}$. The braids $\sigma^{+}_{m,n}$ and $\sigma^{-}_{m,n}$ are schematically shown in Figure 2.14. In particular,

$$\sigma^{+}_{m,0} = \sigma^{-}_{m,0} = \sigma^{+}_{0,m} = \sigma^{-}_{0,m} = 1_m$$

for all $m \geq 1$. It is clear that $(\sigma^{\varepsilon}_{m,n})^{-1} = \sigma^{-\varepsilon}_{n,m}$ for all m, n, and ε.

It is convenient to introduce the symbols $\sigma^{+}_{0,0}, \sigma^{-}_{0,0}$, and 1_0; they all represent an "empty braid on zero strings" $\emptyset$, which satisfies the identities $\emptyset \otimes \alpha = \alpha \otimes \emptyset = \alpha$ for any genuine braid α.

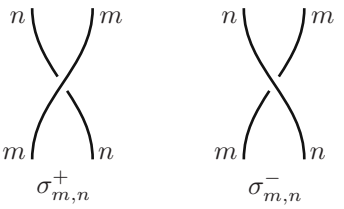

Fig. 2.14. The braids $\sigma^+_{m,n}$, $\sigma^-_{m,n} \in B_{m+n}$

Lemma 2.11. *For any integers $m, n \geq 0$, $r, t \geq 1$, signs $\varepsilon, \nu = \pm$, and braids $\alpha \in B_{n+r}$, $\beta \in B_{n+t}$, $\gamma \in B_{m+t}$, $\delta \in B_{m+r}$, consider the braid*

$$\langle \alpha, \beta, \gamma, \delta \,|\, \varepsilon, \nu \rangle = (1_m \otimes \alpha \otimes 1_t)(1_{m+n} \otimes \sigma^{\nu}_{t,r})(1_m \otimes \beta \otimes 1_r)(\sigma^{-\varepsilon}_{n,m} \otimes 1_{t+r})$$
$$\times (1_n \otimes \gamma \otimes 1_r)(1_{n+m} \otimes \sigma^{-\nu}_{r,t})(1_n \otimes \delta \otimes 1_t)(\sigma^{\varepsilon}_{m,n} \otimes 1_{r+t}) \in B_{m+n+r+t}.$$

Then the M-equivalence class of $\langle \alpha, \beta, \gamma, \delta \,|\, \varepsilon, \nu \rangle$ does not depend on ε, ν, and

$$\langle \alpha, \beta, \gamma, \delta \,|\, \varepsilon, \nu \rangle \sim \langle \delta, \gamma, \beta, \alpha \,|\, \varepsilon, \nu \rangle. \tag{2.3}$$

The reader is encouraged to draw the braid $\langle \alpha, \beta, \gamma, \delta \,|\, \varepsilon, \nu \rangle$ for $\varepsilon = \nu = +$. We shall draw the closure of this braid using the following conventions. Let us think of braid diagrams as lying in a square $I \times I \subset \mathbf{R} \times I$ with inputs on the top side $I \times \{0\}$ and outputs on the bottom side $I \times \{1\}$. The standard orientation on the strands of a braid diagram runs from the inputs to the outputs. We can rotate the square $I \times I$ around its center by the angle $\pi/2$. Rotating $I \times I$ by the angle $\pi/2$ counterclockwise (resp. clockwise), we transform any picture a in $I \times I$ into a picture in $I \times I$ denoted by a_+ (resp. a_-). If a is a braid diagram, then the inputs and outputs of a_+, a_- lie on the vertical sides of the square. Note also that $a_{++} = a_{--}$, where $a_{++} = (a_+)_+$ and $a_{--} = (a_-)_-$.

Pick certain diagrams of the braids $\alpha, \beta, \gamma, \delta$, which we denote by the same letters $\alpha, \beta, \gamma, \delta$, respectively. A little contemplation should persuade the reader that Figure 2.15 represents the closure of the braid $\langle \alpha, \beta, \gamma, \delta \,|\, +, + \rangle$.

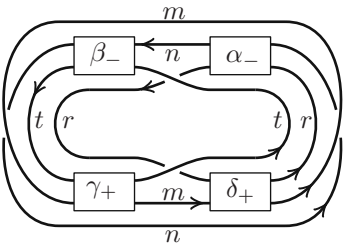

Fig. 2.15. The closure of $\langle \alpha, \beta, \gamma, \delta \,|\, +, + \rangle$

The rest of the proof of Theorem 2.8 goes as follows. In Section 2.6 we deduce this theorem from Lemma 2.11. In Section 2.7 we prove Lemma 2.11. These two sections use different techniques and can be read in any order.

Exercise 2.5.1. Verify that the braids $\langle \alpha, \beta, \gamma, \delta \,|\, \varepsilon, \nu \rangle$ and $\langle \alpha, \beta, \gamma, \delta \,|\, -\varepsilon, -\nu \rangle$ have isotopic closures. Verify that

$$\langle \alpha, \beta, \gamma, \delta \,|\, \varepsilon, \nu \rangle \sim_c \langle \gamma, \delta, \alpha, \beta \,|\, -\varepsilon, -\nu \rangle \,. \tag{2.4}$$

(Hint: Rotate the closed braid in Figure 2.15 through 180°.)

Exercise 2.5.2. Verify (2.3) for $m = n = 0$.

2.6 Deduction of Markov's theorem from Lemma 2.11

We begin by introducing an additional Markov move.

2.6.1 The move M_3

By definition, the second Markov move M_2 transforms a braid $\beta \in B_n$ into $\sigma_n^{\varepsilon}(\beta \otimes 1_1)$ with $\varepsilon = \pm 1$. We define another move M_3 on braids transforming $\beta \in B_n$ into $\sigma_1^{\varepsilon}(1_1 \otimes \beta) \in B_{n+1}$. One can check directly that M_3 preserves the isotopy class of the closure.

Lemma 2.12. *The move* M_3 *expands as a composition of the moves* M_1, M_2.

Proof. Recall the braid $\Delta_n \in B_n$ defined in Section 1.3.3. By formula (1.8),

$$\Delta_n \sigma_i \Delta_n^{-1} = \sigma_{n-i} \in B_n \tag{2.5}$$

for all $n \geq 1$ and all $i = 1, \ldots, n-1$. In particular, $\Delta_{n+1}\sigma_1\Delta_{n+1}^{-1} = \sigma_n \in B_{n+1}$. Taking the inverses in B_{n+1}, we obtain

$$\Delta_{n+1}\sigma_1^{\varepsilon}\Delta_{n+1}^{-1} = \sigma_n^{\varepsilon} \tag{2.6}$$

for $\varepsilon = \pm 1$. We check now that for any $\beta \in B_n$,

$$\Delta_{n+1}(1_1 \otimes \beta)\Delta_{n+1}^{-1} = \Delta_n \beta \Delta_n^{-1} \otimes 1_1 \,. \tag{2.7}$$

Both sides of (2.7) are multiplicative with respect to β, so that it suffices to verify (2.7) for $\beta = \sigma_i \in B_n$, where $i = 1, \ldots, n-1$. We have

$$1_1 \otimes \sigma_i = \sigma_{i+1} \in B_{n+1}$$

and

$$\Delta_{n+1}(1_1 \otimes \sigma_i)\Delta_{n+1}^{-1} = \Delta_{n+1}\sigma_{i+1}\Delta_{n+1}^{-1} = \sigma_{(n+1)-(i+1)} = \sigma_{n-i} \in B_{n+1} \,.$$

At the same time, $\Delta_n \sigma_i \Delta_n^{-1} = \sigma_{n-i} \in B_n$ and

$$\Delta_n \sigma_i \Delta_n^{-1} \otimes 1_1 = \sigma_{n-i} \in B_{n+1}\,.$$

This proves (2.7). Multiplying (2.6) and (2.7), we obtain

$$\Delta_{n+1} \sigma_1^{\varepsilon} (1_1 \otimes \beta) \Delta_{n+1}^{-1} = \sigma_n^{\varepsilon} (\Delta_n \beta \Delta_n^{-1} \otimes 1_1)$$

or, equivalently,

$$\sigma_1^{\varepsilon} (1_1 \otimes \beta) = \Delta_{n+1}^{-1} \sigma_n^{\varepsilon} (\Delta_n \beta \Delta_n^{-1} \otimes 1_1) \Delta_{n+1}\,.$$

Hence M_3 is a composition of the conjugation by Δ_n with M_2 and with the conjugation by Δ_{n+1}^{-1}. □

This lemma implies that the moves $\mathrm{M}_1, \mathrm{M}_2, \mathrm{M}_3$ generate the same equivalence relation $\sim$ on the set $\amalg_{n \geq 1} B_n$ as $\mathrm{M}_1, \mathrm{M}_2$.

2.6.2 Reduction of Theorem 2.8 to Claim 2.15

We now reformulate Theorem 2.8 in terms of closed braids in the solid torus $V \subset \mathbf{R}^3$. Let $\widehat{\mathrm{M}}_2$ be the transformation of closed braids in V replacing the closure of a braid β on n strings with the closure of $\sigma_n^{\varepsilon}(\beta \otimes 1_1)$, where $\varepsilon = \pm 1$. Let $\widehat{\mathrm{M}}_3$ be the transformation of closed braids in V replacing the closure of a braid β on n strings with the closure of $\sigma_1^{\varepsilon}(1_1 \otimes \beta)$, where $\varepsilon = \pm 1$. The moves inverse to $\widehat{\mathrm{M}}_2$, $\widehat{\mathrm{M}}_3$ are denoted by $\widehat{\mathrm{M}}_2^{-1}$, $\widehat{\mathrm{M}}_3^{-1}$, respectively. By Theorem 2.1, to prove Theorem 2.8 it suffices to prove the following assertion.

Claim 2.13. *Two closed braids in V representing isotopic oriented links in $\mathbf{R}^3$ can be related by a sequence of moves $\widehat{\mathrm{M}}_2^{\pm 1}, \widehat{\mathrm{M}}_3^{\pm 1}$ and isotopies in V.*

Here and below all sequences of moves are finite. In Claim 2.13, by isotopy in V we mean a move replacing a closed braid in V with a closed braid in V isotopic to the first one in the class of oriented links in V.

We can reformulate Claim 2.13 in terms of closed braid diagrams in the annulus, as defined in Section 2.2.5. Let $\widetilde{\mathrm{M}}_2$ (resp. $\widetilde{\mathrm{M}}_3$) be the transformation of closed braid diagrams replacing the closure of a braid diagram β on n strands with the closure of $\sigma_n^{\varepsilon}(\beta \otimes 1_1)$ (resp. of $\sigma_1^{\varepsilon}(1_1 \otimes \beta)$), where $\varepsilon = \pm 1$. The moves $\widetilde{\mathrm{M}}_2, \widetilde{\mathrm{M}}_3$ are just the moves $\widehat{\mathrm{M}}_2, \widehat{\mathrm{M}}_3$ restated in terms of diagrams. The moves on closed braid diagrams inverse to $\widetilde{\mathrm{M}}_2, \widetilde{\mathrm{M}}_3$ are denoted by $\widetilde{\mathrm{M}}_2^{-1}, \widetilde{\mathrm{M}}_3^{-1}$, respectively. Recall the braidlike Reidemeister moves Ω_2^{br}, Ω_3^{br}; see Sections 2.1.3 and 2.2.5. To prove Claim 2.13 it suffices to prove the following.

Claim 2.14. *Two closed braid diagrams in an annulus $A \subset \mathbf{R}^2$ representing isotopic oriented links in $\mathbf{R}^3$ can be related by a sequence of moves $(\Omega_2^{\mathrm{br}})^{\pm 1}$, $(\Omega_3^{\mathrm{br}})^{\pm 1}$, $\widetilde{\mathrm{M}}_2^{\pm 1}, \widetilde{\mathrm{M}}_3^{\pm 1}$ and isotopies in the class of oriented link diagrams in A.*

The isotopies here should begin and end with closed braid diagrams in A (with their canonical orientation), but the intermediate oriented link diagrams in A are not required to be closed braid diagrams.

We shall now reduce Claim 2.14 to another claim formulated in terms of so-called 0-diagrams. We use the notation and the terminology introduced in Section 2.4. A 0-*diagram* is an oriented link diagram $\mathcal{D}$ in $\mathbf{R}^2$ such that $h(\mathcal{D}) = 0$ and all the Seifert circles of $\mathcal{D}$ are oriented counterclockwise. These conditions imply that the Seifert circles of $\mathcal{D}$ form a system of concentric circles in $\mathbf{R}^2$. These circles can be numbered by $1, 2, \ldots, n(\mathcal{D})$ counting from the smallest (innermost) circle toward the biggest (outermost) one. Note that the braidlike moves $\Omega_2^{\mathrm{br}}, \Omega_3^{\mathrm{br}}$ transform 0-diagrams into 0-diagrams. The move Ω_1 adding a kink on the left or on the right of a 0-diagram, generally speaking, does not yield a 0-diagram. (Here the left side and the right side of a diagram are determined by its orientation and the counterclockwise orientation in $\mathbf{R}^2$.) However, for any 0-diagram $\mathcal{D}$, the Ω_1-move adding a left kink at a point of $\mathcal{D}$ lying on the innermost Seifert circle yields a 0-diagram $\mathcal{D}'$. The kink becomes the innermost Seifert circle of $\mathcal{D}'$. Such a transformation $\mathcal{D} \mapsto \mathcal{D}'$ is denoted by Ω_1^{int}. Similarly, adding a right kink at a point of $\mathcal{D}$ lying on its outermost Seifert circle and then pushing the kink across the point $\infty \in S^2$ so that it encircles this point, we obtain again a 0-diagram $\mathcal{D}''$ in $\mathbf{R}^2$. The kink becomes the outermost Seifert circle of this diagram. Such a transformation $\mathcal{D} \mapsto \mathcal{D}''$ is denoted by Ω_1^{ext}. In the sequel, by Ω-*moves* on 0-diagrams we mean the transformations Ω_2^{br}, Ω_3^{br}, Ω_1^{int}, Ω_1^{ext}, the inverse transformations, and isotopies in $\mathbf{R}^2$.

Claim 2.15. *Two* 0*-diagrams in* $\mathbf{R}^2$ *representing isotopic oriented links in* $\mathbf{R}^3$ *can be related by a sequence of* Ω*-moves.*

This claim implies Claim 2.14. To see this, note first that closed braid diagrams in an annulus $A \subset \mathbf{R}^2$ are 0-diagrams and for them, $\Omega_1^{\mathrm{int}} = \widetilde{\mathrm{M}}_2$ and $\Omega_1^{\mathrm{ext}} = \widetilde{\mathrm{M}}_3$. Consider now two closed braid diagrams $\mathcal{C}, \mathcal{D}$ in A representing isotopic oriented links in $\mathbf{R}^3$. By Claim 2.15, there is a sequence of 0-diagrams $\mathcal{C} = \mathcal{C}_1, \mathcal{C}_2, \ldots, \mathcal{C}_m = \mathcal{D}$ in $\mathbf{R}^2$ such that each $\mathcal{C}_{i+1}$ is obtained from $\mathcal{C}_i$ by an Ω-move. The construction in the proof of Lemma 2.6 shows that each $\mathcal{C}_i$ is isotopic to a closed braid diagram $\mathcal{B}_i$ in A. It is clear that if $\mathcal{C}_{i+1}$ is obtained from $\mathcal{C}_i$ by $(\Omega_2^{\mathrm{br}})^{\pm 1}$, $(\Omega_3^{\mathrm{br}})^{\pm 1}$, $(\Omega_1^{\mathrm{int}})^{\pm 1}$, $(\Omega_1^{\mathrm{ext}})^{\pm 1}$, then $\mathcal{B}_{i+1}$ is obtained from $\mathcal{B}_i$ by $(\Omega_2^{\mathrm{br}})^{\pm 1}$, $(\Omega_3^{\mathrm{br}})^{\pm 1}$, $\widetilde{\mathrm{M}}_3^{\pm 1}, \widetilde{\mathrm{M}}_2^{\pm 1}$, respectively. A little thinking shows that if $\mathcal{C}_{i+1}$ is obtained from $\mathcal{C}_i$ by an isotopy in $\mathbf{R}^2$, then $\mathcal{B}_{i+1}$ is obtained from $\mathcal{B}_i$ by an isotopy in A. This yields Claim 2.14.

2.6.3 Reduction to Lemma 2.17

Recall the isotopies, bendings, and tightenings of link diagrams as defined in Sections 2.1.2 and 2.4.2. The proof of Claim 2.15 begins with the following lemma.

Lemma 2.16. *Let $\mathcal{E}$, $\mathcal{E}'$ be 0-diagrams in $\mathbf{R}^2$ representing isotopic oriented links in $\mathbf{R}^3$. Then there is a sequence of 0-diagrams $\mathcal{E} = \mathcal{E}_1, \mathcal{E}_2, \ldots, \mathcal{E}_m = \mathcal{E}'$ such that for all $i = 1, 2, \ldots, m-1$, the diagram $\mathcal{E}_{i+1}$ is obtained from $\mathcal{E}_i$ by an Ω-move or by a sequence of bendings, tightenings, and isotopies in the sphere $S^2 = \mathbf{R}^2 \cup \{\infty\}$.*

Proof. Since $\mathcal{E}, \mathcal{E}'$ represent isotopic links, they can be related by a sequence of the following oriented Reidemeister moves: (a) $\Omega_1^{\pm 1}$, (b) $(\Omega_2^{\mathrm{br}})^{\pm 1}$, $(\Omega_3^{\mathrm{br}})^{\pm 1}$, isotopies in $\mathbf{R}^2$, (c) nonbraidlike moves $\Omega_2^{\pm 1}$. Note that the intermediate diagrams created by these moves may have positive height. We will transform this sequence of moves into another one consisting only of bendings, tightenings, isotopies in S^2, and Ω-moves on 0-diagrams.

Recall from Section 2.4.2 that a nonbraidlike move Ω_2 involving two distinct Seifert circles is a bending. A nonbraidlike move Ω_2 involving only one Seifert circle can be obtained as a composition of two Ω_1, a bending, and a tightening; see Figure 2.16. Therefore we can assume that in our sequence of moves, all moves of type (c) are bendings and tightenings.

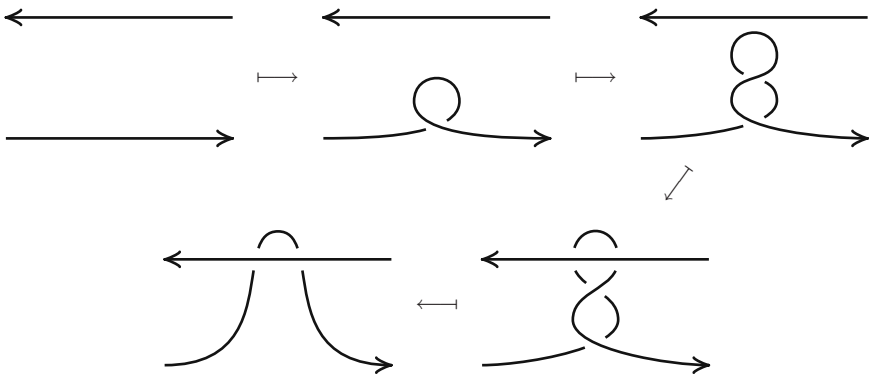

Fig. 2.16. An expansion of Ω_2

Let g be a transformation of type (b) in our sequence applied to a link diagram $\mathcal{D}$ with $h(\mathcal{D}) > 0$. Note that g preserves the set of Seifert circles of the diagram and therefore preserves its height. Since $h(\mathcal{D}) > 0$, the diagram $\mathcal{D}$ has a defect face. We can choose a reduction arc in this face disjoint from the disk where g changes $\mathcal{D}$. Let r be the corresponding bending of $\mathcal{D}$. Clearly, the transformations r and g on $\mathcal{D}$ commute. We replace the transformation $\mathcal{D} \mapsto g(\mathcal{D})$ in our sequence with the sequence

$$\mathcal{D} \xrightarrow{r} r(\mathcal{D}) \xrightarrow{g} gr(\mathcal{D}) \xrightarrow{r^{-1}} r^{-1}gr(\mathcal{D}) = g(\mathcal{D}).$$

The operation g is now performed at a lower height. Gradually we can go all the way down to height zero. Thus we can replace g with a sequence of

bendings, tightenings, and a single move of type (b), say g', on a diagram, $\mathcal{D}'$, of height 0. If the Seifert circles of $\mathcal{D}'$ are oriented counterclockwise, then $\mathcal{D}'$ is a 0-diagram and g' is an Ω-move. If the Seifert circles of $\mathcal{D}'$ are oriented clockwise, then we expand g' as a composition of an isotopy of S^2 transforming $\mathcal{D}'$ into a 0-diagram (cf. the proof of Lemma 2.6), an Ω-move on the latter diagram, and the inverse isotopy.

Let $g = \Omega_1$ be an operation of type (a) in our sequence applied to a link diagram $\mathcal{D}$ in $\mathbf{R}^2$. Inserting bendings and tightenings as above, we can assume that $h(\mathcal{D}) = 0$. Conjugating if necessary g by an isotopy of S^2, we can assume that the Seifert circles of $\mathcal{D}$ are oriented counterclockwise, i.e., that $\mathcal{D}$ is a 0-diagram in $\mathbf{R}^2$. Suppose that the kink added by g to a branch a of $\mathcal{D}$ lies to its left. If a lies on the first (innermost) Seifert circle of $\mathcal{D}$, then $g = \Omega_1^{\mathrm{int}}$. If a lies on the mth Seifert circle of $\mathcal{D}$ with $m \geq 2$, then we apply $m-1$ moves Ω_2^{br} to push a under $m-1$ smaller Seifert circles of $\mathcal{D}$ inside the disk bounded by the innermost Seifert circle. Then we apply Ω_1^{int} on a and push the resulting kink back under the first $m-1$ Seifert circles to the place where the original move $g = \Omega_1$ must have been applied. This pushing should be performed carefully: one first pushes all the $m-1$ Seifert circles in question over the crossing created by Ω_1^{int}. This amounts to $m-1$ moves

$$d_1^+ d_2^{\pm} d_1^- \ \mapsto \ d_2^- d_1^{\pm} d_2^+$$

analyzed in the proof of Theorem 1.6. (This analysis shows that these moves are compositions of $(\Omega_2^{\mathrm{br}})^{\pm 1}, (\Omega_3^{\mathrm{br}})^{\pm 1}$.) After that, one pushes these $m-1$ Seifert circles over the remaining part of the kink, which amounts to $m-1$ tightenings. The resulting chain of moves, schematically shown in Figure 2.17, transforms $\mathcal{D}$ into the same diagram $g(\mathcal{D})$ as g itself. Thus, we can replace the move $\mathcal{D} \mapsto g(\mathcal{D})$ with a finite sequence of moves $(\Omega_2^{\mathrm{br}})^{\pm 1}, (\Omega_3^{\mathrm{br}})^{\pm 1}, \Omega_1^{\mathrm{int}}$ on 0-diagrams followed by $m-1$ tightenings. If the kink added by g lies to the right of a, then we proceed as above but push a toward the external (infinite) face of $\mathcal{D}$ in $\mathbf{R}^2$ and then apply Ω_1^{ext}. □

Lemma 2.17. *Two* 0*-diagrams in* $\mathbf{R}^2$ *related by a sequence of bendings, tightenings, and isotopies in* S^2 *can be related by a sequence of* Ω*-moves.*

This lemma together with the previous one implies Claim 2.15 and Theorem 2.8. The rest of the section is devoted to the proof of Lemma 2.17.

2.6.4 Proof of Lemma 2.17, part I

We consider here the simplest case of Lemma 2.17, namely the one in which the sequence relating two 0-diagrams consists solely of isotopies.

Lemma 2.18. *If two* 0*-diagrams are isotopic in* $S^2 = \mathbf{R}^2 \cup \{\infty\}$*, then they are isotopic in* $\mathbf{R}^2$*.*

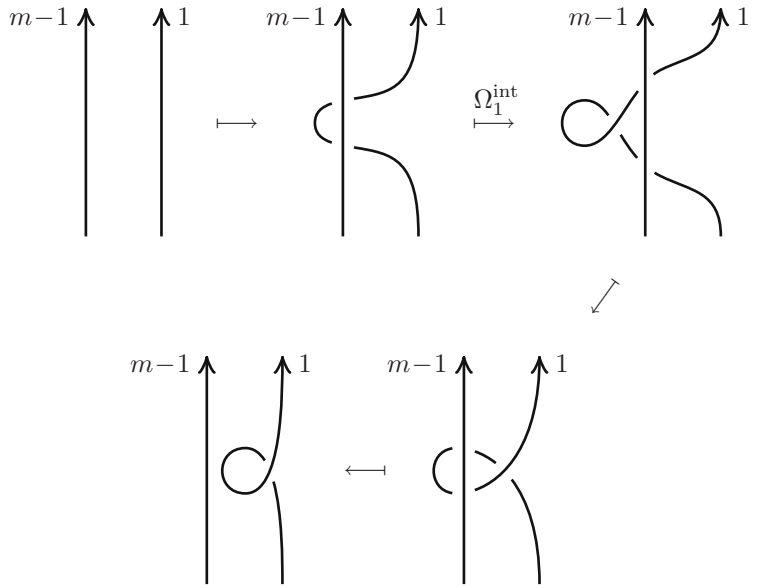

Fig. 2.17. An expansion of Ω_1

Proof. Let $\mathcal{D}, \mathcal{D}'$ be 0-diagrams in $\mathbf{R}^2$ isotopic in S^2. They have then the same number of Seifert circles $N \geq 1$. If $N = 1$, then $\mathcal{D}, \mathcal{D}'$ are embedded circles in $\mathbf{R}^2$ oriented counterclockwise. By the Jordan curve theorem, any embedded circle in $\mathbf{R}^2$ bounds a disk. This implies that such a circle is isotopic to a small metric circle in $\mathbf{R}^2$. Since any two metric circles in $\mathbf{R}^2$, endowed with counterclockwise orientation, are isotopic in $\mathbf{R}^2$, the same holds for $\mathcal{D}, \mathcal{D}'$.

Suppose that $N \geq 2$. Since $\mathcal{D}$, $\mathcal{D}'$ are isotopic in S^2, there is a continuous family of homeomorphisms $\{F_t : S^2 \to S^2\}_{t \in I}$ such that $F_0 = \mathrm{id}$ and F_1 transforms $\mathcal{D}$ into $\mathcal{D}'$. By continuity, all the homeomorphisms F_t are orientation preserving. The Seifert circles of $\mathcal{D}$ split S^2 into $N - 1$ annuli and two disks $D_i = D_i(\mathcal{D})$ and $D_o = D_o(\mathcal{D})$ bounded by the innermost and the outermost Seifert circles of $\mathcal{D}$, respectively. Recall that $S^2 = \mathbf{R}^2 \cup \{\infty\}$ is oriented counterclockwise and so are all Seifert circles of $\mathcal{D}$. It is clear that the orientation of the innermost Seifert circle ∂D_i is compatible with the orientation of D_i induced from the one on S^2. On the other hand, the orientation of the outermost Seifert circle ∂D_o is incompatible with the orientation of D_o induced from the one on S^2. This implies that $F_1 : S^2 \to S^2$ necessarily transforms $D_i(\mathcal{D})$ into $D_i(\mathcal{D}')$ and $D_o(\mathcal{D})$ into $D_o(\mathcal{D}')$ (and not the other way round).

We have $\infty \in D_o(\mathcal{D})$ and therefore $F_1(\infty) \in D_o(\mathcal{D}')$. Hence, there is a closed 2-disk B in the complement of $\mathcal{D}'$ in S^2 containing the points ∞ and $F_1(\infty)$. Pushing $F_1(\infty)$ toward ∞ inside B, we obtain a continuous family of homeomorphisms $\{g_t : S^2 \to S^2\}_{t \in I}$ such that $g_0 = \mathrm{id}$, $g_1(F_1(\infty)) = \infty$, and all g_t are equal to the identity outside B (cf. the proof of Lemma 1.26).

Then $g_1F_1(\mathcal{D}) = g_1(\mathcal{D}') = \mathcal{D}'$ and the one-parameter family of homeomorphisms $\{g_tF_t : S^2 \to S^2\}_{t\in I}$ relates $g_0F_0 = \mathrm{id}$ with g_1F_1. Thus, g_1F_1 is isotopic to the identity in the class of self-homeomorphisms of S^2. By Exercise 1.7.1, g_1F_1 is isotopic to the identity in the class of self-homeomorphisms of S^2 keeping fixed the point ∞. Restricting all homeomorphisms in such an isotopy to $\mathbf{R}^2 = S^2 - \{\infty\}$, we obtain an isotopy of $\mathcal{D}$ into $\mathcal{D}'$ in $\mathbf{R}^2$. □

2.6.5 Proof of Lemma 2.17, part II

Consider a sequence of moves as in Lemma 2.17. By a general position argument, we can assume that the intermediate diagrams created by these moves lie in $\mathbf{R}^2 = S^2 - \{\infty\}$. We will denote bendings and tightenings by arrows pointing in the direction of a lower height. Thus, the notation $\mathcal{C} \overset{s}{\leftarrow} \mathcal{D} \overset{s'}{\rightarrow} \mathcal{C}'$ means that the link digram $\mathcal{C}$ is transformed into $\mathcal{D}$ by a tightening, inverse to a bending s of $\mathcal{D}$, and $\mathcal{D}$ is transformed into $\mathcal{C}'$ by a bending s'. Note that $h(\mathcal{C}) = h(\mathcal{C}') = h(\mathcal{D}) - 1$, so that the height function h has a local maximum at $\mathcal{D}$. We call such a sequence $\mathcal{C} \overset{s}{\leftarrow} \mathcal{D} \overset{s'}{\rightarrow} \mathcal{C}'$ a *local maximum*. Our strategy will be to replace local maxima by (longer) sequences at a lower height.

For a local maximum $\mathcal{C} \overset{s}{\leftarrow} \mathcal{D} \overset{s'}{\rightarrow} \mathcal{C}'$, consider the reduction arcs of s and s'. By a general position argument, we can assume that for all local maxima in our sequence of moves, these two arcs have distinct endpoints and meet transversely in a finite number of points. This number is denoted by $s \cdot s'$.

Lemma 2.19. *For any local maximum $\mathcal{C} \overset{s}{\leftarrow} \mathcal{D} \overset{s'}{\rightarrow} \mathcal{C}'$ with $s \cdot s' \neq 0$, there is a sequence of bendings and tightenings*

$$\mathcal{C} = \mathcal{C}_1 \overset{s_1}{\longleftarrow} \mathcal{D}_1 \overset{s_1'}{\longrightarrow} \mathcal{C}_2 \overset{s_2}{\longleftarrow} \cdots \overset{s_{m-1}'}{\longrightarrow} \mathcal{C}_m \overset{s_m}{\longleftarrow} \mathcal{D}_m \overset{s_m'}{\longrightarrow} \mathcal{C}_{m+1} = \mathcal{C}'$$

such that $s_i \cdot s_i' = 0$ for all i.

Proof. Since the reduction arcs of link diagrams are oriented, we can speak of their left and right sides (with respect to the counterclockwise orientation in $\mathbf{R}^2$). Each reduction arc c of $\mathcal{D}$ can be pushed slightly to the left or to the right, keeping the endpoints on $\mathcal{D}$. This gives disjoint reduction arcs giving rise to the same bending (at least up to isotopy). These arcs are denoted by c_l, c_r, respectively.

Let c, c' be the reduction arcs of s, s', respectively. Let us suppose first that $s \cdot s' \geq 2$. We prove below that there is a reduction arc c'' of $\mathcal{D}$ disjoint from c' and meeting c at fewer than $s \cdot s'$ points. Consider the sequence

$$\mathcal{C} \overset{s}{\longleftarrow} \mathcal{D} \overset{s''}{\longrightarrow} \mathcal{C}'' \overset{s''}{\longleftarrow} \mathcal{D} \overset{s'}{\longrightarrow} \mathcal{C}',$$

where s'' is the bending along c''. We have

$$s \cdot s'' = |c \cap c''| < s \cdot s' \quad \text{and} \quad s' \cdot s'' = |c' \cap c''| = 0\,.$$

Continuing in this way we can reduce the lemma to the case $s \cdot s' = 1$. We now construct c''. Let A, B be distinct points of $c \cap c'$ such that the subarc $AB \subset c$ does not meet c'. Inverting if necessary the orientations of c, c', we can assume that both c and c' are directed from A to B. Assume first that c' crosses c at A from left to right. If c' crosses c at B from right to left, then c'' is obtained by going along c'_l to its intersection point with c_l close to A, then along c_l to its intersection point with c'_l close to B, and then along c'_l. If c' crosses c at B from left to right, then c'' is obtained by going along c'_l to its intersection point with c_r close to A, then along c_r to its intersection point with c'_r close to B, and then along c'_r. It is easy to check that in both cases the arc c'' has the required properties; see Figure 2.18. The case in which c' crosses c at A from right to left is similar.

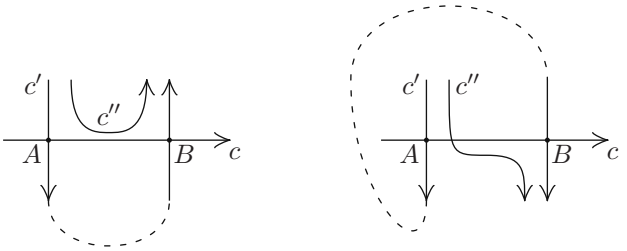

Fig. 2.18. The arc c''

It remains to consider the case $s \cdot s' = 1$. We claim that there is a reduction arc c'' of $\mathcal{D}$ disjoint from $c \cup c'$. Inserting $\mathcal{D} \overset{s''}{\to} \mathcal{C}'' \overset{s''}{\leftarrow} \mathcal{D}$ as above, we will obtain the claim of the lemma. Let O be the unique point of $c \cap c'$ and let f be the face of $\mathcal{D}$ containing c and c' (except their endpoints). Denote the endpoints of c on $\mathcal{D}$ by A_1, A_2. Denote the endpoints of c' on $\mathcal{D}$ by A_3, A_4. Denote by S_i the Seifert circle of $\mathcal{D}$ passing through A_i. By the definition of a reduction arc, $S_1 \neq S_2$ and $S_3 \neq S_4$. Note that the arc $A_1O \cup OA_3$ can be slightly deformed into an arc $c_{1,3}$ in $f - (c \cup c')$ leading from a point on S_1 to a point on S_3. The same arc with opposite orientation is denoted by $c_{3,1}$. We similarly define arcs $c_{1,4}$ and $c_{4,1}$; see Figure 2.19.

If two of the circles S_1, S_2, S_3, S_4 coincide, say $S_1 = S_4$, then the circles $S_1 = S_4$ and $S_3 \neq S_4$ are distinct. Since c' is a reduction arc, they are incompatible. Hence $c'' = c_{1,3}$ is a reduction arc satisfying our requirements.

Thus, we can assume that the circles S_1, S_2, S_3, S_4 are all distinct. Their topological position in $S^2 = \mathbf{R}^2 \cup \{\infty\}$ is uniquely determined: they are boundaries of four disjoint disks in S^2 meeting the crosslike graph $c \cup c'$ at its four endpoints. If S_1 and S_3 are incompatible, then $c_{1,3}$ is a reduction arc in $f - (c \cup c')$ and we are done. Assume that S_1 is compatible with S_3. Since S_4 is incompatible with S_3, the circle S_1 is compatible with S_4 as well. Note that the arcs $c_{1,3}$ and $c_{1,4}$ are not reduction arcs.

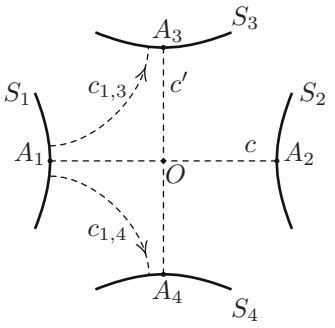

Fig. 2.19. The arcs c, c' and the circles S_1, S_2, S_3, S_4

Recall the disjoint segments γ_x connecting the Seifert circles of $\mathcal{D}$, where x runs over the crossings of $\mathcal{D}$ (see Figure 2.12). The orientation arguments show that the endpoints of each such γ_x necessarily lie on different but compatible Seifert circles. We now distinguish three cases.

Case (i): there are no segments γ_x attached to S_1. A reduction arc of $\mathcal{D}$ connecting S_3 to S_4 is obtained by first following $c_{3,1}$ to a point close to S_1, then encircling S_1 and finally moving along $c_{1,4}$. Since there are no γ_x attached to S_1, this arc lies in $f - (c \cup c')$.

Case (ii): the segments γ_x attached to S_1 connect it to one and the same Seifert circle S. Suppose first that $S \neq S_3$. A reduction arc c'' connecting S_3 to S in $f - (c \cup c')$ is obtained by first following $c_{3,1}$ to a point close to S_1, then encircling S_1 until hitting for the first time a segment γ_x attached to S_1, and then going close to this γ_x until meeting S. If $S = S_3$, then $S \neq S_4$ and we can apply the same construction with S_3 replaced by S_4.

Case (iii): the segments γ_x attached to S_1 connect it to at least two different Seifert circles. We can find two of these segments γ_1, γ_2 with endpoints e_1, e_2 on S_1 such that their second endpoints lie on different Seifert circles and the arc $d \subset S_1 - \{A_1\}$ connecting e_1 to e_2 is disjoint from all the other γ_x attached to S_1. Then a small deformation of the arc $\gamma_1 \cup d \cup \gamma_2$ gives a reduction arc c'' of $\mathcal{D}$ disjoint from $c \cup c'$. □

Lemma 2.20. *For a local maximum $\mathcal{C} \overset{s}{\leftarrow} \mathcal{D} \overset{s'}{\rightarrow} \mathcal{C}'$ with $s \cdot s' = 0$, there are sequences of isotopies in S^2 and bendings $\mathcal{C} \to \cdots \to \mathcal{C}_*$, $\mathcal{C}' \to \cdots \to \mathcal{C}'_*$ such that $\mathcal{C}_* = \mathcal{C}'_*$ or $\mathcal{C}_*, \mathcal{C}'_*$ are 0-diagrams in $\mathbf{R}^2$ related by Ω-moves.*

Proof. Let c, c' be the reduction arcs of the bendings s, s' on $\mathcal{D}$. The assumption $s \cdot s' = 0$ implies that c and c' are disjoint. Hence the bendings s and s' are performed in disjoint areas of the plane and commute with each other. Suppose that they involve different pairs of Seifert circles of $\mathcal{D}$ (these pairs may have one common circle). Then c' is a reduction arc for $\mathcal{C} = s(\mathcal{D})$ and c is a reduction arc for $\mathcal{C}' = s'(\mathcal{D})$. Let $\mathcal{D}'$ be the link diagram obtained by bending $\mathcal{C}$ along c' or, equivalently, by bending $\mathcal{C}'$ along c. The sequences $\mathcal{C} \to \mathcal{D}'$ and $\mathcal{C}' \to \mathcal{D}'$ satisfy the conditions of the lemma.

Suppose from now on that s and s' involve the same (distinct and incompatible) Seifert circles S_1, S_2 of $\mathcal{D}$. Assume that $\mathcal{D}$ has a reduction arc c_1 disjoint from $c \cup c'$ and involving another pair of Seifert circles. Then the bendings s, s', s_1 along c, c', c_1, respectively, commute with each other. The sequences $\mathcal{C} \stackrel{s_1}{\to} \mathcal{C}_1 \stackrel{s'}{\to} \mathcal{D}'$, $\mathcal{C}' \stackrel{s_1}{\to} \mathcal{C}'_1 \stackrel{s}{\to} \mathcal{D}'$ satisfy the conditions of the lemma.

Suppose from now on that all reduction arcs of $\mathcal{D}$ disjoint from $c \cup c'$ involve the Seifert circles S_1, S_2. We choose notation so that c is directed from S_1 to S_2. Assume first that c' is directed from S_1 to S_2. The circles S_1, S_2 bound in S^2 disjoint 2-disks D_1, D_2, respectively. The arcs c, c' lie in the annulus $S^2 - (D_1^\circ \cup D_2^\circ)$ bounded by $S_1 \cup S_2$. These arcs split this annulus into two topological 2-disks D_3, D_4 where $D_3 \cap D_4 = c \cup c'$.

Observe that the Seifert circles of $\mathcal{D}$ distinct from S_1, S_2 are disjoint from $S_1 \cup S_2 \cup c \cup c'$. Therefore the Seifert circles of $\mathcal{D}$ can be partitioned into four disjoint families: the circles lying in D_1, those in D_2, those in the interior of D_3, and those in the interior of D_4. The first two families include $S_1 = \partial D_1$ and $S_2 = \partial D_2$, while the other two families may be empty. To analyze the position of Seifert circles in D_1, note that a reduction arc of $\mathcal{D}$ lying in D_1 is disjoint from $c \cup c'$ or can be made disjoint from $c \cup c'$ by a small deformation near its endpoints. Since such an arc cannot meet S_2, our assumptions imply that $\mathcal{D}$ has no reduction arcs in D_1. The same argument as in the proof of Lemma 2.6 shows that the Seifert circles of $\mathcal{D}$ lying in D_1 form a system of $t \geq 1$ concentric compatible circles with the external circle being S_1. This system of t concentric circles with the same orientation is schematically represented in Figure 2.20 by the left oval. Similar arguments show that the Seifert circles of $\mathcal{D}$ lying in D_2 (resp. in D_3, D_4) form a system of $r \geq 1$ (resp. $n \geq 0, m \geq 0$) concentric circles with the same orientation, represented in Figure 2.20 by the right (resp. upper, lower) oval. The diagram $\mathcal{D}$ is recovered from these four systems of concentric circles by inserting certain braids $\alpha \in B_{n+r}, \beta \in B_{n+t}, \gamma \in B_{m+t}, \delta \in B_{m+r}$ as in Figure 2.20, where we use the notation $\alpha_-, \beta_-, \gamma_+, \delta_+$ introduced after the statement of Lemma 2.11.

Since S_1, S_2 are incompatible they must have the same orientation (clockwise or counterclockwise). For concreteness, we assume that they are oriented counterclockwise. (The case of the clockwise orientation can be reduced to this one by reversing the orientations on $\mathcal{C}, \mathcal{D}, \mathcal{C}'$.) The circles of the other two families are then oriented clockwise: otherwise we can easily find a reduction arc connecting S_1 to one of these circles and disjoint from $c \cup c'$.

Recall that the diagram $\mathcal{C}$ is obtained from $\mathcal{D}$ by a bending s that pushes (a subarc of) S_1 toward S_2 along c and then above S_2. Consider a "superbending" along c pushing the whole band of t circles on the left along c and then over the r right circles. This superbending is a composition of rt bendings, the first of them being s. Moreover, to the resulting link diagram we can apply one more superbending along the arc in S^2 going from the bottom point of the diagram $\mathcal{D}$ down to ∞ and then from ∞ down to the top point of $\mathcal{D}$. (It is of

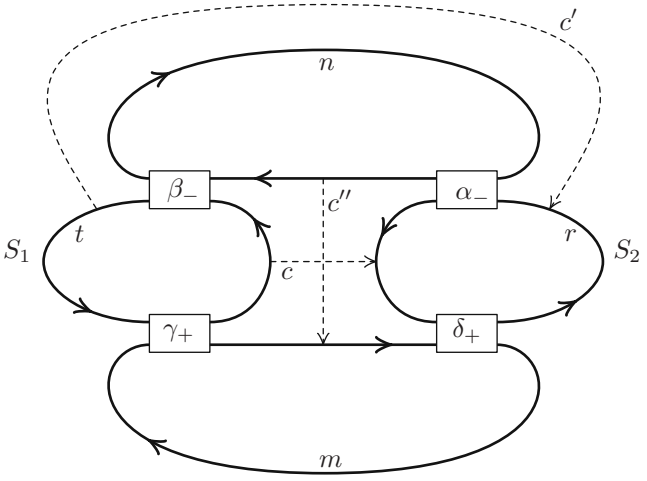

Fig. 2.20. The diagram $\mathcal{D}$

course important that we consider diagrams in S^2 so that reduction arcs and isotopies in S^2 are allowed.)

Performing these two superbendings on $\mathcal{D}$, we obtain the link diagram $\mathcal{C}_*$ drawn in Figure 2.15. (Actually, it is easier to observe the converse, i.e., that $\mathcal{C}_*$ produces $\mathcal{D}$ via two supertightenings inverse to the superbendings described above.) A remarkable although obvious fact is that $\mathcal{C}_*$ is a closed braid diagram and in particular a 0-diagram. In the notation of Lemma 2.11, $\mathcal{C}_*$ represents the closure of the braid $\langle \alpha, \beta, \gamma, \delta \,|\, +, + \rangle$. As we saw, there is a sequence of $rt + mn$ bendings $\mathcal{D} \xrightarrow{s} \mathcal{C} \to \cdots \to \mathcal{C}_*$ in S^2.

Similarly, we can apply a superbending to $\mathcal{D}$ along the arc c', oriented from S_1 to S_2, and then another superbending along the short vertical segment c'' leading from the bottom point of the upper oval toward the top point of the lower oval in Figure 2.20. This gives a link diagram isotopic to the link diagram $\mathcal{C}'_{**}$ drawn on the left of Figure 2.21. (Again, it is easier to check that the inverse moves transform $\mathcal{C}'_{**}$ into $\mathcal{D}$.) As above, there is a sequence of $rt + mn$ bendings $\mathcal{D} \xrightarrow{s'} \mathcal{C}' \to \cdots \to \mathcal{C}'_{**}$ in S^2.

The diagram $\mathcal{C}'_{**}$ looks like a closed braid diagram, but not quite because its Seifert circles are oriented clockwise. Pushing the lower part of $\mathcal{C}'_{**}$ across $\infty \in S^2$, we obtain that $\mathcal{C}'_{**}$ is isotopic in S^2 to a closed braid diagram $\mathcal{C}'_*$ drawn on the right of Figure 2.21. This diagram represents the closure of $\langle \delta, \gamma, \beta, \alpha \,|\, +, + \rangle$. By (2.3), the braids $\langle \alpha, \beta, \gamma, \delta \,|\, +, + \rangle$ and $\langle \delta, \gamma, \beta, \alpha \,|\, +, + \rangle$ are M-equivalent. Therefore the diagrams $\mathcal{C}_*$ and $\mathcal{C}'_*$, representing the closures of these braids, are related by Ω-moves. This gives the sequences of bendings and isotopies $\mathcal{C} \to \cdots \to \mathcal{C}_*$ and $\mathcal{C}' \to \cdots \to \mathcal{C}'_{**} \to \mathcal{C}'_*$ satisfying the requirements of the lemma.

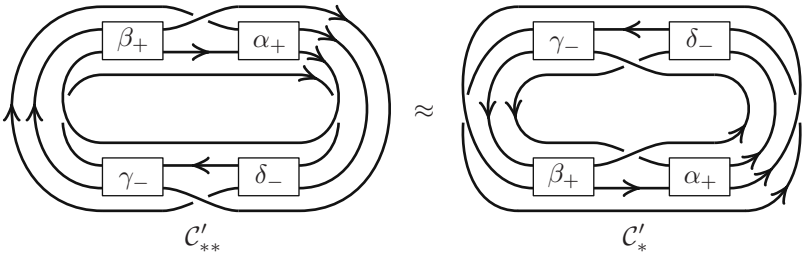

Fig. 2.21. The diagrams $\mathcal{C}'_{**}$ and $\mathcal{C}'_{*}$

If c' is directed from S_2 to S_1, then the argument is similar, though $\langle \delta, \gamma, \beta, \alpha \,|\, +, + \rangle$ should be replaced with $\langle \delta, \gamma, \beta, \alpha \,|\, +, - \rangle$. By the first claim of Lemma 2.11, this does not change the M-equivalence class of the braid. This completes the proof of Lemma 2.20. □

2.6.6 Proof of Lemma 2.17, part III

By the *height* of a sequence of bendings, tightenings, and isotopies on link diagrams in S^2, we mean the maximal height of the diagrams appearing in this sequence. We prove the lemma by induction on the height m of the sequence relating two 0-diagrams in $\mathbf{R}^2$.

If $m = 0$, then the sequence consists solely of isotopies in S^2. In this case Lemma 2.17 follows directly from Lemma 2.18.

Assume that $m > 0$. It is clear that a transformation of a link diagram in S^2 obtained as an isotopy followed by a bending (resp. a tightening) can be also obtained as a bending (resp. a tightening) followed by an isotopy. Therefore all isotopies in our sequence of bendings, tightenings, and isotopies in S^2 can be accumulated at the end of the sequence. In particular, all diagrams of height m in this sequence appear as local maxima, i.e., are obtained by tightening from the previous diagram and yield the next diagram by bending. Lemma 2.19 shows that we can replace our sequence with another one that connects the same initial and terminal 0-diagrams, has the same height m, and additionally satisfies the condition that $s \cdot s' = 0$ in all its local maxima $\mathcal{C} \overset{s}{\leftarrow} \mathcal{D} \overset{s'}{\rightarrow} \mathcal{C}'$. By Lemma 2.20, for each such local maximum, there is a sequence of isotopies, bendings, and tightenings

$$\mathcal{C} \to \cdots \to \mathcal{C}_* \sim \mathcal{C}'_* \leftarrow \cdots \leftarrow \mathcal{C}' \,,$$

where $\sim$ stands for the coincidence $\mathcal{C}_* = \mathcal{C}'_*$ or for Ω-moves transforming $\mathcal{C}_*$ into $\mathcal{C}'_*$ (which are then 0-diagrams). The height of all link diagrams in this sequence is less than or equal to $h(\mathcal{C}) = h(\mathcal{C}') < h(\mathcal{D}) \leq m$. Replacing every local maximum $\mathcal{C} \overset{s}{\leftarrow} \mathcal{D} \overset{s'}{\rightarrow} \mathcal{C}'$ by such a sequence, we obtain a concatenation of sequences of height $\leq m-1$ with sequences of Ω-moves on 0-diagrams. By the induction assumption, this implies the claim of the lemma. □

2.7 Proof of Lemma 2.11

We begin by introducing a useful involution $\beta \mapsto \overline{\beta}$ on the set of braids.

2.7.1 The involution $\beta \mapsto \overline{\beta}$

For a braid $\beta \in B_n$, set $\overline{\beta} = \Delta_n \beta \Delta_n^{-1} \in B_n$, where $\Delta_n \in B_n$ is the braid defined in Section 1.3.3. Since Δ_n^2 lies in the center of B_n, the automorphism $\beta \mapsto \overline{\beta}$ of B_n is an involution. Formula (2.5) implies that if

$$\beta = \sigma_{i_1}^{r_1} \sigma_{i_2}^{r_2} \cdots \sigma_{i_m}^{r_m}$$

with $1 \leq i_1, i_2, \ldots, i_m \leq n-1$ and $r_1, r_2, \ldots, r_m \in \mathbf{Z}$, then

$$\overline{\beta} = \sigma_{n-i_1}^{r_1} \sigma_{n-i_2}^{r_2} \cdots \sigma_{n-i_m}^{r_m} .$$

This formula implies that a diagram of $\overline{\beta}$ can be obtained from a diagram of β in $\mathbf{R} \times I = \mathbf{R} \times I \times \{0\}$ by rotating about the line $\{(n+1)/2\} \times \mathbf{R} \times \{0\}$ in $\mathbf{R}^3$ by the angle π. This geometric description of the involution $\beta \mapsto \overline{\beta}$ shows that $\overline{\alpha \otimes \beta} = \overline{\beta} \otimes \overline{\alpha}$ for any braids $\alpha \in B_m$ and $\beta \in B_n$. Note for the record that $\overline{\alpha\beta} = \overline{\alpha}\overline{\beta}$ for any $\alpha, \beta \in B_n$ and $\overline{1_n} = 1_n$. It is easy to deduce from the definitions that $\overline{\sigma_{m,n}^{\varepsilon}} = \sigma_{n,m}^{\varepsilon}$ for any $m, n \geq 0$ and $\varepsilon = \pm$.

Lemma 2.21. *If two braids β, β' are M-equivalent, then the braids $\overline{\beta}, \overline{\beta'}$ are M-equivalent.*

Proof. We have $\overline{\beta} \sim_c \beta \sim \beta' \sim_c \overline{\beta'}$. □

2.7.2 Ghost braids

We introduce a class of ghost braids. Let $\mu \in B_{n+k}$ with $n \geq 1, k \geq 0$. We say that μ is *n-right-ghost* and write $\mu \equiv 1_n$ if for any $m \geq 0$ and any $\beta \in B_{m+n}$, we have $(\beta \otimes 1_k)(1_m \otimes \mu) \sim \beta$; see Figure 2.22. Examples of right-ghost braids will be given below. Taking $m = 0$, $\beta = 1_n$, we conclude that $\mu \equiv 1_n \Rightarrow \mu \sim 1_n$. (The converse is in general not true.)

Given an n-right-ghost braid $\mu \in B_{n+k}$, we define a move (a transformation) on braids, denoted by $M(\mu)$. For any $m \geq 0$, $\alpha, \beta \in B_{m+n}$, $\rho \in B_m$, the move $M(\mu)$ transforms $\beta(\rho \otimes 1_n)\alpha$ into $(\beta \otimes 1_k)(\rho \otimes \mu)(\alpha \otimes 1_k)$; see Figure 2.23. The inverse transformation replaces the factor $\rho \otimes \mu$ with $\rho \otimes 1_n$ and deletes 1_k on the right of the other factors. The move $M(\mu)$ and its inverse preserve the M-equivalence class of the braid. Indeed,

$$\begin{aligned}
\beta(\rho \otimes 1_n)\alpha &\sim_c \alpha\beta(\rho \otimes 1_n) \\
&\sim (\alpha\beta(\rho \otimes 1_n) \otimes 1_k)(1_m \otimes \mu) \\
&= (\alpha \otimes 1_k)(\beta \otimes 1_k)(\rho \otimes 1_{n+k})(1_m \otimes \mu) \\
&= (\alpha \otimes 1_k)(\beta \otimes 1_k)(\rho \otimes \mu) \\
&\sim_c (\beta \otimes 1_k)(\rho \otimes \mu)(\alpha \otimes 1_k) .
\end{aligned}$$

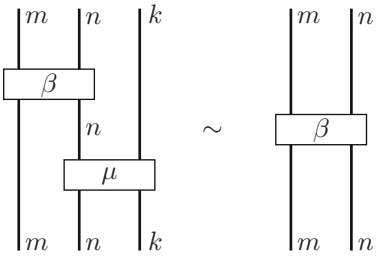

Fig. 2.22. The formula $(\beta \otimes 1_k)(1_m \otimes \mu) \sim \beta$

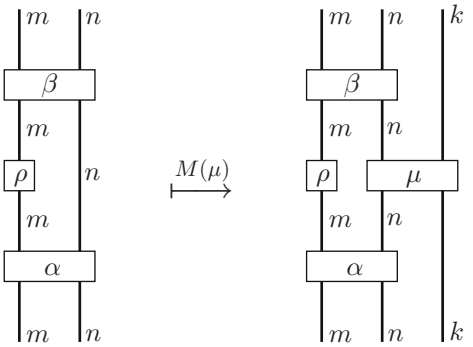

Fig. 2.23. The transformation $M(\mu)$

Given a braid $\mu \in B_{n+k}$ with $n \geq 1, k \geq 0$, we say that μ is *n-left-ghost* and write $\mu \equiv' 1_n$ if $(1_k \otimes \beta)(\mu \otimes 1_m) \sim \beta$ for any $m \geq 0$, $\beta \in B_{n+m}$. For any such μ and any $\alpha, \beta \in B_{n+m}$, $\rho \in B_m$, we denote by $M'(\mu)$ the move transforming $\beta(1_n \otimes \rho)\alpha$ into $(1_k \otimes \beta)(\mu \otimes \rho)(1_k \otimes \alpha)$. An argument similar to the one above shows that this move and its inverse preserve the M-equivalence class of the braid.

Lemma 2.22. *Let $\mu \in B_{n+k}$ with $n \geq 1, k \geq 0$. If $\mu \equiv 1_n$, then $\overline{\mu} \equiv' 1_n$.*

Proof. Pick $\beta \in B_{n+m}$ with $m \geq 0$ and set $\gamma = (1_k \otimes \beta)(\overline{\mu} \otimes 1_m)$. We must verify that $\gamma \sim \beta$. Obviously, $\gamma \sim_c \overline{\gamma} = (\overline{\beta} \otimes 1_k)(1_m \otimes \mu)$. Since $\mu \equiv 1_n$, we have $(\overline{\beta} \otimes 1_k)(1_m \otimes \mu) \sim \overline{\beta} \sim_c \beta$. Therefore $\gamma \sim \beta$. □

For $n \geq 1$, set $\theta_n^+ = \Delta_n^2 \in B_n$ and $\theta_n^- = \Delta_n^{-2} \in B_n$. Clearly, for any $\varepsilon = \pm$,

$$\overline{\theta_n^\varepsilon} = \Delta_n \theta_n^\varepsilon \Delta_n^{-1} = \theta_n^\varepsilon \,.$$

As an exercise, the reader may check that

$$\theta_n^\varepsilon = (\theta_{n-1}^\varepsilon \otimes 1_1)\, \sigma_{1,n-1}^\varepsilon \sigma_{n-1,1}^\varepsilon = \sigma_{1,n-1}^\varepsilon (1_1 \otimes \theta_{n-1}^\varepsilon)\, \sigma_{n-1,1}^\varepsilon \,. \tag{2.8}$$

The following lemma provides key examples of ghost braids. The proof of this lemma is given in an algebraic form. Here and below, the reader is strongly encouraged to draw the pictures corresponding to our formulas.

Lemma 2.23. *For any $n \geq 1$ and $\varepsilon = \pm$, set*

$$\mu_{n,\varepsilon} = (1_n \otimes \theta_n^{-\varepsilon})\, \sigma_{n,n}^{\varepsilon} = \sigma_{n,n}^{\varepsilon}(\theta_n^{-\varepsilon} \otimes 1_n) \in B_{2n}\,.$$

Then

$$\overline{\mu}_{n,\varepsilon} = (\theta_n^{-\varepsilon} \otimes 1_n)\, \sigma_{n,n}^{\varepsilon} = \sigma_{n,n}^{\varepsilon}(1_n \otimes \theta_n^{-\varepsilon}) \in B_{2n}$$

and $\mu_{n,\varepsilon} \equiv 1_n$, $\overline{\mu}_{n,\varepsilon} \equiv 1_n$, $\mu_{n,\varepsilon} \equiv' 1_n$, $\overline{\mu}_{n,\varepsilon} \equiv' 1_n$.

Proof. We shall represent θ_n^{ε} graphically by a box with ε inside. Two pictorial representations of $\mu_{n,-}$ are given in Figure 2.24. Pictures of $\mu_{n,+}$ are obtained by exchanging the over/undercrossings and replacing $+$ by $-$ in the box.

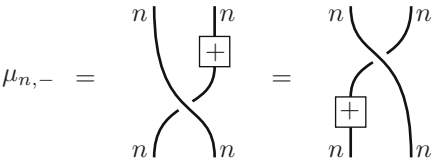

Fig. 2.24. The braid $\mu_{n,-}$

The expansions for $\overline{\mu}_{n,\varepsilon}$ in the statement of the lemma are obtained from the expansions for $\mu_{n,\varepsilon}$ and the geometric interpretation of the involution $\mu \mapsto \overline{\mu}$. By Lemma 2.22, the formulas $\mu_{n,\varepsilon} \equiv 1_n$, $\overline{\mu}_{n,\varepsilon} \equiv 1_n$ will imply that $\mu_{n,\varepsilon} \equiv' 1_n$, $\overline{\mu}_{n,\varepsilon} \equiv' 1_n$. To prove that $\mu_{n,\varepsilon}$ is n-right-ghost, we must verify that

$$(\beta \otimes 1_n)(1_m \otimes \mu_{n,\varepsilon}) \sim \beta$$

for any $\beta \in B_{m+n}$ with $m \geq 0$. Clearly,

$$\begin{aligned}(\beta \otimes 1_n)(1_m \otimes \mu_{n,\varepsilon}) &= (\beta \otimes 1_n)(1_m \otimes 1_n \otimes \theta_n^{-\varepsilon})(1_m \otimes \sigma_{n,n}^{\varepsilon}) \\ &= (\beta \otimes \theta_n^{-\varepsilon})(1_m \otimes \sigma_{n,n}^{\varepsilon}) \\ &\sim_c (1_m \otimes \sigma_{n,n}^{\varepsilon})(\beta \otimes \theta_n^{-\varepsilon})\,.\end{aligned}$$

It remains to prove that

$$(1_m \otimes \sigma_{n,n}^{\varepsilon})(\beta \otimes \theta_n^{-\varepsilon}) \sim \beta\,. \tag{2.9}$$

The formula $\overline{\mu}_{n,\varepsilon} \equiv 1_n$ also follows from (2.9), since

$$\begin{aligned}(\beta \otimes 1_n)(1_m \otimes \overline{\mu}_{n,\varepsilon}) &\sim_c (1_m \otimes \overline{\mu}_{n,\varepsilon})(\beta \otimes 1_n) \\ &= (1_m \otimes \sigma_{n,n}^{\varepsilon})(1_{m+n} \otimes \theta_n^{-\varepsilon})(\beta \otimes 1_n) \\ &= (1_m \otimes \sigma_{n,n}^{\varepsilon})(\beta \otimes \theta_n^{-\varepsilon})\,.\end{aligned}$$

The proof of the equality (2.9) goes by induction on n. For $n = 1$, we have $\theta_n^{-\varepsilon} = 1_1$ and $1_m \otimes \sigma_{n,n}^{\varepsilon} = \sigma_{m+1}^{\varepsilon}$, where $\sigma_{m+1}^{+} = \sigma_{m+1}$ and $\sigma_{m+1}^{-} = \sigma_{m+1}^{-1}$.

The transformation $\sigma_{m+1}^{\varepsilon}(\beta \otimes 1_1) \mapsto \beta$ is an inverse Markov move. Therefore, formula (2.9) holds for $n = 1$. In the inductive step we shall use the identity

$$\sigma_{n,n}^{\varepsilon} = (\sigma_{n-1,n}^{\varepsilon} \otimes 1_1)(1_{n-1} \otimes \sigma_{1,n}^{\varepsilon})\,.$$

For $n > 1$,

$$\begin{aligned}
&(1_m \otimes \sigma_{n,n}^{\varepsilon})(\beta \otimes \theta_n^{-\varepsilon}) \\
&\quad = (1_m \otimes \sigma_{n,n}^{\varepsilon})(1_m \otimes 1_n \otimes \theta_n^{-\varepsilon})(\beta \otimes 1_n) \\
&\quad = (1_m \otimes \theta_n^{-\varepsilon} \otimes 1_n)(1_m \otimes \sigma_{n,n}^{\varepsilon})(\beta \otimes 1_n) \\
&\quad = (1_m \otimes \theta_n^{-\varepsilon} \otimes 1_n)(1_m \otimes \sigma_{n-1,n}^{\varepsilon} \otimes 1_1)(1_{m+n-1} \otimes \sigma_{1,n}^{\varepsilon})(\beta \otimes 1_n) \\
&\quad \sim_c (1_{m+n-1} \otimes \sigma_{1,n}^{\varepsilon})(\beta \otimes 1_n)(1_m \otimes \theta_n^{-\varepsilon} \otimes 1_n)(1_m \otimes \sigma_{n-1,n}^{\varepsilon} \otimes 1_1) \\
&\quad = (1_{m+2n-2} \otimes \sigma_{1,1}^{\varepsilon})(1_{m+n-1} \otimes \sigma_{1,n-1}^{\varepsilon} \otimes 1_1) \\
&\qquad \times (\beta \otimes 1_n)(1_m \otimes \theta_n^{-\varepsilon} \otimes 1_n)(1_m \otimes \sigma_{n-1,n}^{\varepsilon} \otimes 1_1) \\
&\quad \sim (1_{m+n-1} \otimes \sigma_{1,n-1}^{\varepsilon})(\beta \otimes 1_{n-1})(1_m \otimes \theta_n^{-\varepsilon} \otimes 1_{n-1})(1_m \otimes \sigma_{n-1,n}^{\varepsilon})\,,
\end{aligned}$$

where the last transformation is M_2^{-1}. The resulting braid is a conjugate of

$$\begin{aligned}
&(1_m \otimes \theta_n^{-\varepsilon} \otimes 1_{n-1})(1_m \otimes \sigma_{n-1,n}^{\varepsilon})(1_{m+n-1} \otimes \sigma_{1,n-1}^{\varepsilon})(\beta \otimes 1_{n-1}) \\
&\quad = (1_m \otimes \theta_n^{-\varepsilon} \otimes 1_{n-1})(1_m \otimes \sigma_{1,n-1}^{\varepsilon} \otimes 1_{n-1})(1_m \otimes \sigma_{n-1,n}^{\varepsilon})(\beta \otimes 1_{n-1}) \\
&\quad = (1_m \otimes \theta_n^{-\varepsilon} \sigma_{1,n-1}^{\varepsilon} \otimes 1_{n-1})(1_m \otimes \sigma_{n-1,n}^{\varepsilon})(\beta \otimes 1_{n-1})\,.
\end{aligned}$$

Substituting in the latter braid the expansion

$$\theta_n^{-\varepsilon} \sigma_{1,n-1}^{\varepsilon} = \theta_n^{-\varepsilon} (\sigma_{n-1,1}^{-\varepsilon})^{-1} = \sigma_{1,n-1}^{-\varepsilon} (1_1 \otimes \theta_{n-1}^{-\varepsilon})\,,$$

which follows from (2.8), we obtain

$$\begin{aligned}
&(1_m \otimes \sigma_{1,n-1}^{-\varepsilon} \otimes 1_{n-1})(1_{m+1} \otimes \theta_{n-1}^{-\varepsilon} \otimes 1_{n-1})(1_m \otimes \sigma_{n-1,n}^{\varepsilon})(\beta \otimes 1_{n-1}) \\
&\qquad = (1_m \otimes \sigma_{1,n-1}^{-\varepsilon} \otimes 1_{n-1})(1_m \otimes \sigma_{n-1,n}^{\varepsilon})(\beta \otimes \theta_{n-1}^{-\varepsilon}) \\
&\qquad \sim_c (1_m \otimes \sigma_{n-1,n}^{\varepsilon})(\beta \otimes \theta_{n-1}^{-\varepsilon})(1_m \otimes \sigma_{1,n-1}^{-\varepsilon} \otimes 1_{n-1}) \\
&\qquad = (1_{m+1} \otimes \sigma_{n-1,n-1}^{\varepsilon})(1_m \otimes \sigma_{n-1,1}^{\varepsilon} \otimes 1_{n-1}) \\
&\qquad\quad \times (\beta \otimes \theta_{n-1}^{-\varepsilon})(1_m \otimes \sigma_{1,n-1}^{-\varepsilon} \otimes 1_{n-1}) \\
&\qquad = (1_{m+1} \otimes \sigma_{n-1,n-1}^{\varepsilon})\,(\beta' \otimes \theta_{n-1}^{-\varepsilon})\,,
\end{aligned}$$

where

$$\beta' = (1_m \otimes \sigma_{n-1,1}^{\varepsilon})\,\beta\,(1_m \otimes \sigma_{1,n-1}^{-\varepsilon})\,.$$

By the induction assumption,

$$\begin{aligned}
(1_{m+1} \otimes \sigma_{n-1,n-1}^{\varepsilon})\,(\beta' \otimes \theta_{n-1}^{-\varepsilon}) &\sim \beta' \\
&= (1_m \otimes \sigma_{n-1,1}^{\varepsilon})\beta(1_m \otimes \sigma_{n-1,1}^{\varepsilon})^{-1} \sim_c \beta\,.
\end{aligned}$$

This completes the proof of (2.9) and of the lemma. □

Lemma 2.24. *For any integers $m, n \geq 0$, $r \geq 1$ and braids $\beta \in B_{m+r}$, $\gamma \in B_{m+n}$, the M-equivalence class of the braid*

$$\alpha_\varepsilon = (\beta \otimes 1_n)\,(1_m \otimes \sigma_{n,r}^{\varepsilon})\,(\gamma \otimes 1_r)\,(1_m \otimes \sigma_{r,n}^{-\varepsilon})$$

does not depend on $\varepsilon = \pm$. (Here, if $m = n = 0$, then $\gamma = 1_0$.)

Proof. If $n = 0$, then $\sigma_{n,r}^{+} = \sigma_{n,r}^{-}$ and hence $\alpha_+ = \alpha_-$. If $m = 0$, then $\alpha_+ = \beta \otimes \gamma = \alpha_-$. Suppose that $m \geq 1$ and $n \geq 1$. We shall prove that $\alpha_+ \sim \alpha_-$; see Figure 2.25.

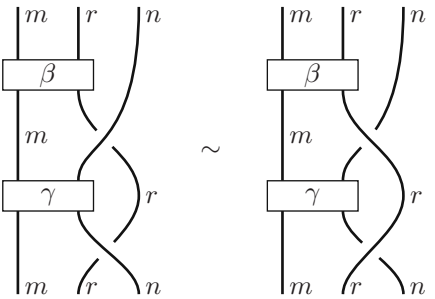

Fig. 2.25. $\alpha_+ \sim \alpha_-$

We first rewrite the factor $1_m \otimes \sigma_{n,r}^{+}$ of α_+ using the obvious expansion

$$1_m \otimes \sigma_{n,r}^{+} = (1_m \otimes \sigma_{n,r}^{+}\sigma_{r,n}^{+})\,(1_{m+r} \otimes 1_n)\,(1_m \otimes \sigma_{n,r}^{-})\,. \tag{2.10}$$

By Lemma 2.23, the M-equivalence class of α_+ is preserved under the transformation replacing the term 1_n in the factor $1_{m+r} \otimes 1_n$ by the braid

$$\overline{\mu}_{n,-} = (\theta_n^{+} \otimes 1_n)\,\sigma_{n,n}^{-} = \sigma_{n,n}^{-}(1_n \otimes \theta_n^{+})$$

and tensoring on the right all the other factors in the expression for α_+ by 1_n. This transforms the right-hand side of (2.10) into the braid

$$\psi = (1_m \otimes \sigma_{n,r}^{+}\sigma_{r,n}^{+} \otimes 1_n)\,(1_{m+r} \otimes \theta_n^{+} \otimes 1_n)\,(1_{m+r} \otimes \sigma_{n,n}^{-})\,(1_m \otimes \sigma_{n,r}^{-} \otimes 1_n)\,.$$

Figure 2.26 shows that $\psi = \psi_1\psi_2\psi_3$, where

$$\psi_1 = 1_{m+r} \otimes \overline{\mu}_{n,-}\,, \quad \psi_2 = 1_m \otimes \sigma_{n,r}^{-} \otimes 1_n\,, \quad \psi_3 = 1_{m+n} \otimes \sigma_{n,r}^{+}\sigma_{r,n}^{+}\,.$$

Therefore,

$$\begin{aligned}
\alpha_+ &\sim (\beta \otimes 1_{2n})\,\psi_1\psi_2\psi_3\,(\gamma \otimes 1_{r+n})\,(1_m \otimes \sigma_{r,n}^{-} \otimes 1_n) \\
&= \psi_1\,(\beta \otimes 1_{2n})\,\psi_2\,(\gamma \otimes 1_{r+n})\,\psi_3\,(1_m \otimes \sigma_{r,n}^{-} \otimes 1_n) \\
&\sim_c (\beta \otimes 1_{2n})\,\psi_2\,(\gamma \otimes 1_{r+n})\,\psi_3\,(1_m \otimes \sigma_{r,n}^{-} \otimes 1_n)\,\psi_1\,.
\end{aligned}$$

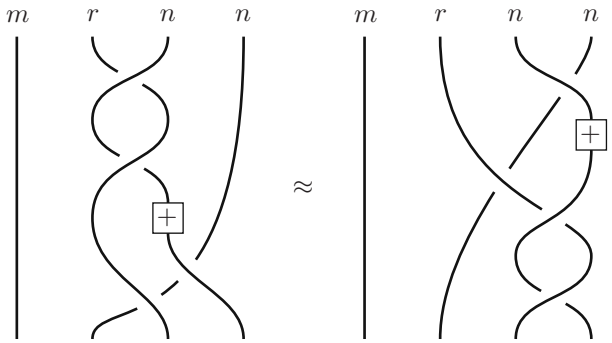

Fig. 2.26. $\psi = \psi_1\psi_2\psi_3$

Drawing pictures, one observes that

$$\psi_3\,(1_m \otimes \sigma^-_{r,n} \otimes 1_n)\,\psi_1 \\ = (1_m \otimes \sigma^-_{r,n} \otimes 1_n)(1_{m+r} \otimes \overline{\mu}_{n,-})(1_m \otimes \sigma^+_{n,r}\sigma^+_{r,n} \otimes 1_n)\,.$$

Thus,

$$\alpha_+ \sim (\beta \otimes 1_{2n})(1_m \otimes \sigma^-_{n,r} \otimes 1_n)(\gamma \otimes 1_{r+n}) \\ \times (1_m \otimes \sigma^-_{r,n} \otimes 1_n)(1_{m+r} \otimes \overline{\mu}_{n,-})(1_m \otimes \sigma^+_{n,r}\sigma^+_{r,n} \otimes 1_n)\,.$$

By Lemma 2.23, we can replace $\overline{\mu}_{n,-}$ with 1_n and simultaneously remove 1_n on the right of the other factors. This and the identity $\sigma^-_{r,n}\sigma^+_{n,r} = 1_{r+n}$ give

$$\alpha_+ \sim (\beta \otimes 1_n)(1_m \otimes \sigma^-_{n,r})(\gamma \otimes 1_r)(1_m \otimes \sigma^+_{r,n}) = \alpha_-\,. \qquad \square$$

Lemma 2.25. *Under the assumptions of Lemma 2.24, the M-equivalence class of the braid*

$$(1_n \otimes \beta)(\sigma^{\varepsilon}_{r,n} \otimes 1_m)(1_r \otimes \gamma)(\sigma^{-\varepsilon}_{n,r} \otimes 1_m)$$

does not depend on $\varepsilon = \pm$.

Proof. This follows from Lemma 2.24 by applying the involution $\mu \mapsto \overline{\mu}$ and using Lemma 2.21. $\square$

2.7.3 Proof of Lemma 2.11

The independence of the sign ε follows from Lemma 2.25, where the symbols $r, n, m, \varepsilon, \beta$, and γ should be replaced respectively with

$$n,\ m,\ t+r,\ -\varepsilon,\ (\alpha \otimes 1_t)(1_n \otimes \sigma^{\nu}_{t,r})(\beta \otimes 1_r),\ (\gamma \otimes 1_r)(1_m \otimes \sigma^{-\nu}_{r,t})(\delta \otimes 1_t)\,.$$

The independence of the sign ν follows from the fact that conjugate braids are M-equivalent and Lemma 2.24, where the symbols $n, m, \varepsilon, \beta, \gamma$ should be replaced respectively with

$$t,\ m+n,\ \nu,\ (1_n \otimes \delta)(\sigma_{m,n}^{\varepsilon} \otimes 1_r)(1_m \otimes \alpha),\ (1_m \otimes \beta)(\sigma_{n,m}^{-\varepsilon} \otimes 1_t)(1_n \otimes \gamma)\,.$$

We now prove (2.3). By the first claim of the lemma, it suffices to consider the case $\varepsilon = \nu$. Consider the braid

$$\langle\!\langle \alpha, \beta, \gamma, \delta \,|\, \varepsilon \rangle\!\rangle = (\alpha \otimes \gamma)(1_n \otimes \sigma_{m,r}^{\varepsilon} \otimes 1_t)(1_n \otimes \theta_m^{\varepsilon} \otimes \sigma_{t,r}^{\varepsilon})(1_n \otimes \sigma_{t,m}^{\varepsilon} \otimes 1_r)$$
$$\times (\beta \otimes \delta)(1_n \otimes \sigma_{m,t}^{-\varepsilon} \otimes 1_r)(1_n \otimes \theta_m^{-\varepsilon} \otimes \sigma_{r,t}^{-\varepsilon})(1_n \otimes \sigma_{r,m}^{-\varepsilon} \otimes 1_t) \in B_{m+n+r+t}\,.$$

Note the obvious conjugacy

$$\langle\!\langle \alpha, \beta, \gamma, \delta \,|\, \varepsilon \rangle\!\rangle \sim_c \langle\!\langle \beta, \alpha, \delta, \gamma \,|\, -\varepsilon \rangle\!\rangle\,. \tag{2.11}$$

We claim that

$$\langle \alpha, \beta, \gamma, \delta \,|\, \varepsilon, \varepsilon \rangle \sim \langle\!\langle \alpha, \beta, \gamma, \delta \,|\, \varepsilon \rangle\!\rangle\,. \tag{2.12}$$

This will imply (2.3) for $\nu = \varepsilon$: applying (2.12), (2.11), and (2.4), we obtain

$$\langle \alpha, \beta, \gamma, \delta \,|\, \varepsilon, \varepsilon \rangle \sim \langle \beta, \alpha, \delta, \gamma \,|\, -\varepsilon, -\varepsilon \rangle \sim \langle \delta, \gamma, \beta, \alpha \,|\, \varepsilon, \varepsilon \rangle\,.$$

The case $\nu = -\varepsilon$ of (2.3) follows then from the first claim of the lemma.

A sequence of moves establishing (2.12) for $\varepsilon = +$ is given pictorially in Figure 2.27. (These moves can be described algebraically, which however is less instructive.) Here, instead of drawing braids we draw their closures. This is more economical in terms of space and does not hinder the argument since conjugate braids are M-equivalent.

The first and the last diagrams in Figure 2.27 represent the closures of the braids $\langle \alpha, \beta, \gamma, \delta \,|\, +, + \rangle$ and $\langle\!\langle \alpha, \beta, \gamma, \delta \,|\, + \rangle\!\rangle$, respectively. The first transformation in Figure 2.27 is a single move $M(\mu_{m,-})$. (It would be more logical to write $+_+$ in the box but we write simply $+$.) The next two moves are isotopies in the class of closed braid diagrams (this amounts to conjugation of braids). Note that the box with $+$ followed by a box with $-$ is just the trivial braid; this splitting of the trivial braid is needed for the next move. The fourth move is the inverse to $M'(\overline{\mu}_{m,-})$. The last move is an isotopy of closed braid diagrams. Since all these moves preserve the M-equivalence class of a braid, we obtain (2.12) for $\varepsilon = +$. The case $\varepsilon = -$ is treated similarly using the mirror image of Figure 2.27. □

Exercise 2.7.1. Verify that the moves M_2, M_3 correspond to each other under the involution $\beta \mapsto \overline{\beta}$ on the set of braids.

Exercise 2.7.2. Let $\mu \in B_{n+k}$ with $n \geq 1, k \geq 0$ be an n-right-ghost braid. Verify that $1_r \otimes \mu \equiv 1_{r+n}$ for any $r \geq 0$ and $(\delta \otimes 1_k)\,\mu\,(\delta^{-1} \otimes 1_k) \equiv 1_n$ for any $\delta \in B_n$.

Solution. For any $\beta \in B_{m+r+n}$ with $m \geq 0$,

$$(\beta \otimes 1_k)(1_m \otimes 1_r \otimes \mu) = (\beta \otimes 1_k)(1_{m+r} \otimes \mu) \sim \beta\,.$$

For any $\beta \in B_{m+n}$ with $m \geq 0$,

$$\begin{aligned}(\beta \otimes 1_k)\big(1_m \otimes (\delta \otimes 1_k)\mu(\delta^{-1} \otimes 1_k)\big)&\\ &= (\beta \otimes 1_k)(1_m \otimes \delta \otimes 1_k)(1_m \otimes \mu)(1_m \otimes \delta^{-1} \otimes 1_k)\\ &\sim_c (1_m \otimes \delta^{-1} \otimes 1_k)(\beta \otimes 1_k)(1_m \otimes \delta \otimes 1_k)(1_m \otimes \mu)\\ &= \big((1_m \otimes \delta^{-1})\beta(1_m \otimes \delta) \otimes 1_k\big)(1_m \otimes \mu)\\ &\sim (1_m \otimes \delta^{-1})\beta(1_m \otimes \delta) \sim_c \beta\,.\end{aligned}$$

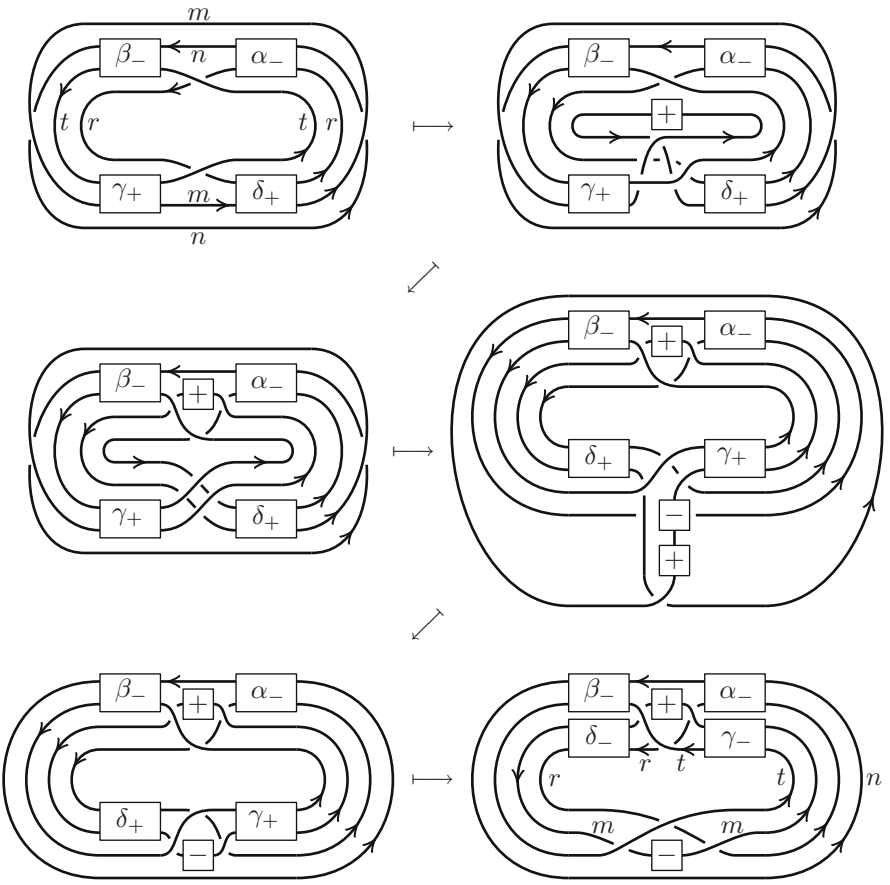

Fig. 2.27. Proof of formula (2.12)

Notes

The content of Section 2.1 is standard. Theorem 2.1 was first pointed out by Artin [Art25] without proof; see also [Mor78, Th. 1], and [BZ85, Prop. 10.16].

Theorem 2.3 is due to Alexander [Ale23a]. The algorithm of Section 2.4.3 transforming a link diagram into a closed braid diagram is due to Vogel [Vog90], who improved a previous construction by Yamada [Yam87]. Bendings were introduced by Vogel (under a different name). The height of a link diagram was introduced by Traczyk [Tra98], who also stated Lemmas 2.4–2.6. Our proof of Lemmas 2.5 and 2.6 is based on arguments from [Vog90, Sect. 5]. Corollary 2.7 is due to Yamada [Yam87]. Exercise 2.4.1 is due to Traczyk [Tra98].

Theorem 2.8 was announced by Markov [Mar36] in 1936. The first published proof appeared in the monograph [Bir74]. According to [Bir74, p. 49], this proof "is based on notes taken at a seminar at Princeton University in 1954. The speaker is unknown to us. . . ." Different proofs were given by Bennequin [Ben83], Morton [Mor86], and Traczyk [Tra98]. The proof of Markov's theorem given above follows Traczyk [Tra98].

http://www.springer.com/978-0-387-33841-5

Braid Groups
Kassel, C.; Turaev, V.
2008, X, 338 p. 60 illus., Hardcover
ISBN: 978-0-387-33841-5